Misregulation of translation drives prostate cancer drug resistance

Emeline I. J. Lelong[1,2], France Hélène Joncas[1,2], Pauline Adjibade[1,2], Valerie ST.-Sauveur Grenier[1,2], Jean-Philippe Lambert[1,2], Paul Toren[1,2,&,*], Rachid Mazroui[1,2,&,*], Samer M. I. Hussein[1,2,&,*]

[1] Laval University Cancer Research Centre;

[2] Research Center of the CHU of Québec – Laval University; Québec, Canada, G1R 3S3

& These authors contributed equally to this work

* *To whom correspondence should be addressed:* Samer.Hussein@crchudequebec.ulaval.ca, Paul.Toren@crchudequebec.ulaval.ca, Rachid.Mazroui@crchudequebec.ulaval.ca

Key words:

Prostate cancer, enzalutamide, resistance, translation, lncRNA

ABSTRACT

Emerging evidence associates translation factors and regulators to tumorigenesis. Recent advances in our ability to perform global translatome analyses indicate that our understanding of translational changes in cancer resistance is still limited. Here, we characterize global translational changes that occur during the acquisition of prostate cancer (PCa) drug resistance. We generated a patient derived xenograft (PDX) model created from PCa cells to recapitulate key features of resistant PCa progression. From an enzalutamide-sensitive patient derived cell line (VCaP), we generated a castration resistant cell line ($VCaP^{CRPC}$) and an enzalutamide resistant cell line ($VCaP^{ER}$). We performed Total and polyribosome-bound RNA sequencing and mass spectroscopy from both $VCaP^{CRPC}$ and $VCaP^{ER}$ to reveal their respective translatomes. We found that in drug-resistant cells, RNAs associated to ribosomes were enriched for nuclear RNA and DNA binding related biological processes, whereas RNAs that are less associated showed enrichment for processes such as cell membrane and cell-cell junction related biological processes. These results were corroborated by mass spectrometry and suggest that translation is indeed affected during drug resistance. Furthermore, our analysis revealed enrichment of long non-coding RNAs associated to ribosomes, which may suggest aberrant translation or translation of novel peptides that can be considered as new biomarkers. Our findings thus point towards novel therapeutic avenues that may target drug-resistant cells.

INTRODUCTION

Following stimuli or a change in their environment, cells need to adjust their protein production through modulation of the translation machinery, in order to ensure proliferation and survival. Translation is a highly regulated process, involving different pathways[1]. Phosphorylation of key translation factors is inhibitory to general translation and can be used by the cell to preserve energy and essential biomolecules, for instance in response to stresses[2]. This leads to specific translation of mRNAs implicated in cell survival[3–5]. While these processes are essential to the response of cells to environmental changes, disturbances in translation regulation is known to lead to the development of various cancers[6–11].

Recently, evidence has shown that cancers could alter translation in order to reduce apoptosis and to increase the production of survival factors[12,13]. Specifically, high expression of translation factors has been associated to high cancer grade and is also associated with an increased risk of metastasis[14]. The main question is how the cancerous cell could face the huge

metabolic requirement. The literature describes a crosstalk between metabolic and translation pathways[15] which are necessary for tumor cell survival. Indeed, increasing glycolytic[16] and fatty acid synthesis programs[17,18], have been found to be implicated in cancer cell, survival to hypoxic environments, hinting at a remodelling of metabolic pathways in cancer cells[19–21]. Also, studies have revealed that tumors cells can rely on different metabolites to respond to their excessive cellular growth need[22]. All this data suggests that translation is important for cancer progression. Consequently, some factors involved in translation are already being used as cancer therapeutic targets[23,24]. Despite all of this information and knowing that proteins are regulated at multiple levels but aren't represented by their RNA's level[25]; efficient systems to validate the dependency of cancers on translation remodelling remain rare and far between. In particular, a paucity of experimental prostate cancer (PCa) has been found, those relevant to study the link between misregulated translation and PCa resistance, for which there is presently no cure.

PCa is the first cancer occurring in men in Canada (https://www.cancer.ca). Following local treatment, 40% of patients suffer from chemical resurgence and metastasis[26–28]. Since a large proportion of metastasis proliferation is dependent on androgen signaling, androgen deprivation therapy (**ADT**) has become the standard treatment for recurrence. For example, in the last ten years, Enzalutamide (**ENZ**), a potent antiandrogen, has been used commonly in androgen receptor (**AR**) targeted therapies. Alas, resistance to ADT inevitably develops for this type of cancer. Correlation between misregulation of translation and cancer resistance have been shown in some studies[14]. Existing clinical data also suggests that PCa resistance may be related to alterations in the translation signaling pathways, which, in turn, can cause differential translation of specific mRNAs. This also suggests a major role of translation regulation in determining protein levels which can drive PCa resistance[5,31,32]. Moreover, these studies are consistent with recent data reporting a regulatory crosstalk between AR and the regulation of translation[29]. This data also suggests that the modifications in the translation pathway which occur during ADT may lead to metastasis by promoting translation of mRNAs involved in tumorigenesis. Unfortunately, studies investigating global translational changes following cancer resistance are still missing today.

In order to unveil perturbations in translation acquired upon PCa resistance acquisition, we developed a method to study targets of pathogenic transcription and translation, merging global analysis of RNAs by RNA-Sequencing (RNA-Seq) and their association to ribosomes through poly(ribo)some profiling in sensitive and resistant PCa cell lines. From an enzalutamide-

sensitive patient derived cell line (VCaP), we generated a castration resistant cell line ($VCaP^{CRPC}$) and an enzalutamide resistant cell line ($VCaP^{ER}$). We used these cell lines in conjunction with other PCa resistance models to perform, to the best of our knowledge, the first detailed analysis of the translatome in resistant PCa. The gene expression profile was studied, and the differentially expressed genes between PCa resistant state were identified. Through Gene Ontology (GO) analysis on RNAs differentially expressed or bound to ribosomes and proteins differentially expressed, we discovered that RNAs associated to ribosomes were enriched for nuclear RNA and DNA binding related biological processes in drug-resistant cells. Whereas RNAs that are less associated showed enrichment for processes such as cell membrane and cell-cell junction related biological processes. These results were corroborated by mass spectrometry and suggest that translation is indeed affected during drug resistance. Furthermore, our analysis revealed enrichment of long non-coding RNAs associated to ribosomes, which may suggest aberrant translation or translation of novel peptides that can be considered as new biomarkers. Our findings thus point towards novel therapeutic targets and key genes which are involved in acquisition of drug resistance and could serve as potential biomarker for prognosis, diagnosis and drug therapies.

RESULTS

Establishment of Enzalutamide resistant cell lines

With the advent of potent AR-agonists (such as ENZ) as first line therapy for CRPC patients, a few groups developed ENZ-resistant cellular models[43-45]. The first and most widely characterized ENZ-resistant cells, named MR49F, were generated through serial passage of LNCaP cells (androgen-sensitive prostate adenocarcinoma cells) in ENZ-treated mice[30]. MR49F cells recapitulate some key features of ENZ-resistant cancer. However, they do not faithfully represent what happens in patients. Aiming to better mimic enzalutamide resistance acquisition in a cellular model, we created our own ENZ-resistant prostate cancer model. Similarly to what was shown in previous publications[30], we first used an ENZ-sensitive prostate cell line : VCaP (Fig. 1A). One million cells were inoculated in male athymic nude mice. Two weeks later, the mice were surgically castrated, mimicking castration treatments offered to patients. Following the development of castration resistance in cells, tumor recurrence was observed. Castration-resistant cells were extracted from theses tumors to establish a new cell line termed $VCaP^{CRPC}$. Mice with castration-resistant tumors were then force-fed with 10mg/kg

ENZ (or vehicle) 5 days per week until tumor recurrence. Cell lines were established from these tumors and named VCaP^{ER} (Fig. 1B). To confirm ENZ resistance acquisition in VCaP^{ER}, we performed proliferation assays for VCaP^{CRPC} and VCaP^{ER} in the presence or absence of ENZ. ENZ treatment negatively affected the proliferation of VCaP^{CRPC} whereas VCaP^{ER} were insensitive (Fig. 1C). This assay confirmed that ENZ-resistance follows ENZ treatment and is not induced by castration (Fig. 1B).

Previous studies have already linked the expression of AR with castration resistance acquisition[31], which was concordant with the moderate amounts of AR detected in VCaP^{CRPC} (Fig. 1C). Interestingly, VCaP^{ER} displayed very high AR expression, as is also observed in cases of ADT[32]. Additionally, AR splice variant AR-V7 has been associated with ENZ resistance acquisition. Similarly to what was previously observed in sensitive LNCaPs, VCaP^{CRPC} do not express AR-V7, while high expression is observed in VCaP^{ER} (Fig. 1C). These first results show that our VCaP-VCaP^{CRPC}-VCaP^{ER} model closely recapitulates the process of cancer resistance acquisition after ENZ treatment.

To understand how transcription and translation is coordinated during resistance acquisition in prostate cancer, we endeavoured to analyze the transcriptome (i..e. total RNA), translatome (i.e. ribosome-bound RNA) and proteome (i.e. total proteins) from the generated cell lines. First, we collected total RNA from VCaP, VCaP^{CRPC} and VCaP^{ER}, and submitted it to RNA-Seq (Fig. 1D). We next performed polysome profiling (P.P.) in both sensitive VCaP^{CRPC} and ENZ-resistant VCaP^{ER}. Heavy polysome fractions were collected and associated RNAs were sequenced (Fig. 1D). Finally, VCaP, VCaP^{CRPC} and VCaP^{ER} proteins were extracted and sent to Mass Spectrometry (M.S.) (Fig. 1E).

Taking advantage of these proteomics and RNA-Seq datasets for both VCaP^{CRPC} and VCaP^{ER}, we sought to determine whether high RNA levels in cells correlated with high RNA association to ribosomes or to protein abundance. Through Pearson correlation coefficient (ρ) analysis, we found that transcriptome and translatome correlated well in both VCaP^{CRPC} and VCaP^{ER} (Fig. S2E-F). We further observed relatively high correlations between transcriptome and proteome in VCaP^{CRPC} and VCaP^{ER} ($\rho = 0.333$ and $\rho = 0.336$ respectively) (Fig. 1E). This suggests that RNA abundance in PCa represents a moderate predictor of protein abundance, and corroborates recent studies showing that in other cancers (breast, ovarian and colorectal), 10 to 20% of variations observed in protein abundance could be explained by mRNA abundance[33–35]. However, transcription of an RNA does not represent a guarantee of protein synthesis. We therefore looked at correlation between translatome and proteome and observed slightly higher

correlation in $VCaP^{CRPC}$ ($\rho = 0.331$) when compared to the ENZ-resistant cell line $VCaP^{ER}$ ($\rho = 0.311$). This modest difference in correlation between ENZ-sensitive and -resistant models hint towards a potential misregulation in translation regulation in prostate cancer resistance.

Differentially gene and pathway enrichment between $VCaP^{ER}$ and $VCaP^{CRPC}$ transcriptomes and translatomes.

To gain a general understanding of the genes and pathways differentially regulated upon acquisition of ENZ-resistance, we first performed differential expression analysis of total and polyribosome RNA-Seq. This yielded 814 RNAs highly bound to ribosomes and 608 RNAs highly expressed exclusively in $VCaP^{ER}$. Moreover, 119 RNAs shared both high expression and high binding to ribosomes. On the other hand, 930 RNAs highly bound to ribosomes and 361 RNAs highly expressed were specific to $VCaP^{CRPC}$, from which 136 RNAs shared both high expression and high binding to ribosomes.

To identify which groups of genes showed differential expression, and to better understand how resistance is acquired in our PCa model, gene ontology (GO) term enrichment analysis was performed on these gene lists using DAVID 6.8[36]. GO term analysis of RNAs highly bound to ribosomes in $VCaP^{ER}$ revealed significantly enriched genes corresponding to the nucleus and centrosome cellular components (GOCC) (Fig. 2C), and in biological processes (GOBP) related to the regulation of transcription. (Fig. S2A). In contrast, we observed that RNAs bound to ribosomes in $VCaP^{CRPC}$ were enriched with GO terms for exosomes and plasma membrane cellular components (Fig. 2C), as well as GOBPs involving calcium ion binding, heparin binding and protein binding (Fig. 2A).

The same analysis was performed for differentially expressed genes (total RNA) in ENZ-sensitive ($VCaP^{CRPC}$) and ENZ-resistant ($VCaP^{ER}$) cells lines. GO-terms analysis both for $VCaP^{CRPC}$ and $VCaP^{ER}$ cells revealed significant enrichment in cell membrane and cytoplasmic GOCCs, including cell-cell adhesion, extracellular exosome and plasma membrane (Fig. 2C). Intriguingly, these results demonstrate a consistent enrichment of GOCCs linked with membrane or cytoplasm, both in highly expressed RNAs and ribosomes-bound RNAs for ENZ-sensitive $VCaP^{CRPC}$ cells, but not for ENZ-resistant $VCaP^{ER}$ cells, for which GO terms enriched with upregulated RNAs and ribosome-bound RNAs do not correlate in terms of cellular components or biological processes.

To further characterize the differentially regulated gene pathways in this ENZ-resistance cellular model, we carried out gene set enrichment analyses (GSEA) on genes which were either

differentially expressed or differentially associated to ribosomes. 268 genes sets were found to be upregulated in VCaP^{ER} total RNA (with 108 downregulated), whereas 79 gene sets were preferentially found associated to ribosomes in VCaP^{ER} (with 189 downregulated in ribosomes) (Fig. 1D and Fig. S2B). We once again observed cytoplasmic and membrane-linked GO terms enriched in total and polysomal RNA of VCaP^{CRPC} and total RNA of VCaP^{ER}, whereas nuclear GO-terms were upregulated in polysomal RNAs in VCaP^{ER} resistant cell line, therefore corroborating the precedent DAVID analyses. Finally, to highlight the differences of transcriptome and translatome regulation previously observed in VCaP^{ER}, we performed Spearman correlation analyses on the enrichment scores of significantly upregulated gene sets. Comparison of transcriptome and translatome in such fashion revealed a greatly decreased correlation between RNA abundance and association to ribosomes in the context of ENZ-resistance (ρ in VCaP^{ER} = 0.333, ρ in VCaP^{CRPC}= 0.462).

Taken together, these results are indicative of perturbations in gene expression at the translational level which might occur during ENZ-resistance acquisition, potentially promoting the resistant phenotype exhibited by VCaP^{ER} cells.

Changes translation genes occur in the proteomic landscape during resistance acquisition

To further characterize protein abundance changes following resistance acquisition, we analyzed differential expression of proteins in our previously generated mass spectrometry datasets (Fig. 1D). Out of the 3002 proteins detected in our prostate cell lines, 2727 were quantifiable (90%). In total, 277 were significantly differentially expressed (DEPs) (9%), including 115 up- and 150 down-regulated proteins in VCaP^{ER}, when compared to VCaP^{CRPC} (Fig. 3A). To identify potential gene groups or pathways implicated in ENZ-resistance, we performed **GSEA** like previously described. VCaP^{ER} proteome reveals enrichment in mitochondrial translation (both elongation and termination). (Fig. 3B). Moreover, network analysis using stringApp on Cytoscape[37] shows that proteins preferentially expressed in the resistant cell line form two distinct clusters : mitochondrial translation and cellular respiration (Fig. 3C). Additionally, two clusters were observed for proteins down-regulated in VCaP^{ER}, showing involvement in translational initiation and RNA metabolism.

To evaluate the importance of these differentially expressed proteins in cancer patient survival, we analyzed publicly available data on cBioPortal[38,39]. We found that alterations in genes coding for identified DEPs in VCaP^{ER} corresponded to significantly lower disease free survival over time in PCa patients. Interestingly, proteins up-regulated in VCaP^{ER} showed much higher

difference between the altered and unaltered groups, as well as a higher significance, when compared to proteins down-regulated in VCaP^{ER}.

To confirm that the proteins highly expressed in VCaPER were indeed linked to resistance, we performed M.S. on an additional ENZ-resistant cell line (MR49F). We observed that proteins highly expressed in VCaP^{ER} corresponded well with those highly expressed in MR49F, which was not the case for proteins highly expressed in VCaP^{CRPC} (Fig. S3B). Taken together, these proteomic analyses reveal important differences in the translated proteins upon acquisition of ENZ resistance in PCa cell lines, and hints at their importance in cancer resistance.

Enzalutamide resistance induces shifts in translation efficiency

To further explore how resistance could affect translation, we next examined translational efficiency (TE) of RNAs, calculated using normalized mRNA abundance and abundance in polysome-bound RNAs ($CPM_{Polysome\ profiling}/CPM_{Total\ RNA}$). As a first observation, several genes show significantly different TE ratios (DTE) in VCaP^{ER} when compared to VCaP^{CRPC} (Fig.4A). We found some genes with high TE ratios implicated in metabolic processes, such as NUDT19, whereas others showing low TE ratio are implicated in cellular adherence, for example BCAM or regulation of translation, such as EIF3D and EIF3I. Looking at GO terms enriched with high or low TE ratio genes in VCaP^{ER} revealed once again that genes exhibiting a high TE ratio are associated with nuclear GO terms (nucleus, nucleoplasm), whereas low TE ratio genes show membrane or cytoplasm go-terms enrichment (cytosol, membrane) (Fig.4B). This further corroborated the previously explored GO terms VCaP^{ER} translatome. However, when looking at VCaP^{ER} differential protein expression, we could find only a few examples of differentially expressed proteins with a corresponding TE ratio (Supplemental Fig.S4A). Therefore, high or low TE ratio does not correspond well to protein expression in VCaP^{ER}.

Interestingly, when comparing whole transcriptome with genes with differential translation efficiency in VCaP^{ER}, we found a shift in TE ratio distributions (median for whole transcriptome =-0.03, median for DTE genes = -0.39) (Fig.4C). DTE genes therefore exhibit a globally lower TE than should be expected. Thus, resistance could cause a reduction in translation efficiency for a subset of genes. To evaluate the importance of these genes in prostate cancer resistance, we analyzed publicly available data on cBioPortal. We found that alterations in genes with high TE ratio in VCaP^{ER} corresponded to significantly lower disease-free survival over time for PCa patients, when compared to genes with low TE ratio (Fig.4D-E). In order to see if some of genes with high TE ratio could act as potential biomarkers, we next investigated

the expression of genes with high TE ratios, first in other cell lines mimicking PCa resistance, but also in PCa patient biopsies. One such example is NUDT19 (Nudix hydrolase 19), a protein involved in metabolism which is both highly expressed, but also shows high TE ratios in $VCaP^{ER}$. Western-Blots show high NUDT19 expression in $VCaP^{ER}$ and MR49F (both resistant to ENZ), but not in $VCaP^{CRPC}$ and LNCaP (both sensitive to ENZ) (Supplemental Fig.S4B). Additionally, high expression of NUDT19 seems to be linked to early recurrence (biochemical reccurence = BCR) in PCa patients (Fig. 4D). Another protein known to be highly expressed in PCa in cases of resistance to enzalutamide or abiroterone is androgen-receptor splice variant 7 (AR-V7)[40,41], an androgen-receptor splice variant. This variant encodes a truncated protein that lacks the C-terminal ligand-binding domain but retains the transactivating N-terminal domain and could therefore constitutively activate downstream target genes involved in PCa progression. AR-V7 expression is higher in advanced PCa, and NUDT19 expression follows the same pattern (Fig.4E). This result reveals that proteins highly expressed and showing high TE ratios could act as powerful biomarkers for PCa resistance.

Aberrant association of lncRNAs to ribosomes may play a role in cancer resistance

Although we have now established TE differences between $VCaP^{ER}$ and $VCaP^{CRPC}$, it remains to be seen whether this affects only specific gene types, such as protein coding genes, or rather globally affects all gene types such as long non-coding RNAs, which have also been shown to bind ribosomes [Ref]. Indeed, when taking genes with differential TE (DTE) indiscriminately, a decrease in TE is seen when compared to the whole gene population (Fig.4C). However, this is not constant in all types of genes. Notably, mRNAs with differential TE (DTE) show a lower TE ratio in $VCaP^{ER}$ (median = -0.41) when compared to all mRNAs (-0.07). Long Non Coding RNAs (lncRNAs) on the other hand, show an inverse pattern : lncRNAs with DTE show a higher TE ratio in $VCaP^{ER}$ (median = 0.51) than all lncRNAs (median = 0.15) (Fig.5A). In fact, resistance seems to be accompanied by an increase in TE ratios for lncRNAs, but also to a higher association of these non-coding genes with ribosomes compared to mRNAs (Supplemental Fig.S6A-B). This finding suggests that lncRNAs could actually be coding or undergo aberrant translation resistant PCa. Indeed, various coding genes are involved in cancer metastasis, proliferation and aggressivity, such as p53 or PTEN (ref), or implicated in translation misregulation, for example, eIF2alpha (Nguyen 2018 ref). However, recent evidence shows that non-coding genes also play a major role in malignancies (ref). To validate this hypothesis, we searched for putative peptides produced from lncRNAs with high TE in publicly available datasets as well as our own. 189 lncRNA-encoded peptides were detected in our cell

lines and others (human induced pluripotent stem cell and fibroblasts). 41 of them exhibited high TE ratios in VCaP^{ER}, while 23 lncRNAs with low TE ratio were also detected (Fig.5B). To evaluate the importance of these lncRNAs in overall survival in PCa patients, we once again turned to cBioPortal. We found that alterations in lncRNAs with high but also low TE ratios have correlate with poor overall survival of patients (Supplemental Fig. S6C). In fact, of the 41 lncRNAs with high TE ratio, 11 show a strong negative correlation with overall survival (Fig.5C), whereas alterations in 3 out of the 23 lncRNAs with low TE ratios also strongly correlated with poor patient outcome (Supplemental Fig.S6D). Hence, alterations in lncRNAs with high TE ratios more often tend to correlate with low overall survival of PCa patients (Fig.5D). We next investigated if alterations in lncRNAs with differential TE ratios could be linked to cancer grade in PCa. Analysis of Gleason scores from PCa patient revealed a high prevalence of alterations in lncRNAs with high TE ratios in medium and high grade cancer (Gleason score between 7 and 9) (Fig.5E). These findings therefore underscore a link between lncRNA TE ratios and their alteration in high grade cancer.

These results drive the hypothesis that elevation of the TE ratios of lncRNAs a could be accompanied by translation of aberrant protein products, which could in turn play a role in prostate cancer resistance and severity. To study how these lncRNAs could be translated to form peptide products in conditions of cancer resistance, we first need to understand why these lncRNAs change their cellular localization. Indeed, most lncRNAs are known to be nuclar. JPX, for instance, has been detected by M.S. in hiPSC (ref) and exhibits a high TE ratio in VCaP^{ER}. However, to be translated, an RNA needs to be located in the cytoplasm. One possibility lies upon the alternative splicing of RNAs, which often results in multiple isoforms with diverse cellular localizations. We therefore asked if these lncRNAs could be the targets of alternative splicing, which could lead to the production of cytoplasmic, and therefore potentially coding isoforms. When looking at splicing for lncRNAs with high TE ratios such as JPX, Linc00467 and WARS_AS1, we detected events of alternative splicing in VCaP^{ER} (Fig.5F & Fig.S6I). JPX presents a variant with alternative splicing of four exons in the VCaP^{ER} translatome, whereas the canonical isoform seems to be restricted to the VCaP^{CRPC} cell line (Fig.5G & Supplemental Fig.S6F). Another lncRNA, Linc00467, shows a switch in isoform expression between VCaP^{CRPC} and VCaP^{ER}, but also an isoform present in both cell lines, but restricted to the polysome-bound RNAs (Fig.5H & Supplemental Fig.S6G).

Altogether, these results show that alternative splicing of lncRNAs could lead variants which could differentially bind to ribosomes, be translated or affect translation of other genes.

Existence of these lncRNA variants could explain the aberrant association to ribosomes which is observed in VCaP^{ER} and grant coding potential to otherwise non-coding genes in the context of PCa resistance.

DISCUSSION

Mounting evidence now shows that cancer resistance can lead to perturbation of translation mechanisms through upregulation or downregulation of certain translation factors, such as mTOR ou eIF2. Moreover, recent publications revealed that mTOR is a promising target for cancer therapy[42]. Despite all of this information, efficient systems to validate the dependency of cancers on translation remodelling remain rare especially since RNA targeted by this translation perturbation are still unknown. Furthermore, despite the fact that prostate cancer is one of the most diagnosed cancers in man, no current therapy exists to overcome drug resistant of this disease.

Here, we performed a thorough analysis of the misregulation of translation during drug resistance acquisition, by generating new cancer resistant cell lines named VCaP^{CRPC} (resistant to castration treatment but sensitive to Enzalutamide) and VCaP^{ER} (resistant to both treatments) from a sensitive cell line VCaP. We found that several RNAs are differentially expressed or/and bound to ribosomes between VCaP^{CRPC} and VCaP^{ER}. Interstingly, we found that the translatome of VCaP^{ER} correlated slightly less with its proteome than VCaP^{CRPC}, suggesting a difference in translation regulation in drug-resistant cells. Upon further investigation of the proteome, we found that the main pathways misregulated in VCaP^{ER} cells are genes implicated in translation, that being mitochondrial translation, translation initiation or translation elongation. We demonstrate that genes upregulated in VCaP^{ER} cells correlate with a worse outcome mainly for disease progression if altered or mutated, although these alterations do not affect the expression of these genes (data not shown). These results demonstrate that our study provides a good model for addressing drug resistance, where we also show that the main genes implicated in drug resistance are genes affecting mitochondrial translation and metabolism. Indeed, therapeutic agents targeting mitochondrial processes have shown promise in inhibiting prostate cancer cell progression[43–46]. We also show that certain ribosomal genes, for example RPL9 and RPS13, and translation factors, for example EIF4B, are downregulated in our model compared to other studies implicating translation in prostate cancer progression[4729,48] and to other models, such as the TRAMP mouse model for prostate adenocarcinoma (Verma et al. Frontiers 2019). In these

models, several of these genes are actually upregulated. This difference in results may be due to the fact that we model a progression towards drug resistance. Furthermore, the downregulation of genes implicated in translation may suggest that current therapeutics targeting translation may have a detrimental effect on PCa progression in patients leading to drug resistance.

Our study also highlights translation misregulation is not limited to protein coding genes, but also affects non-coding genes. In fact, we demonstrate that the translation efficiency is negatively affected in protein coding genes, which may be explained by the downregulation of translation factors in VCaP^{ER} cells. However, this does not explain the overall increase in ribosome bound lncRNAs and the positive shift in translation efficiency for lncRNAs. It has been shown that lncRNAs may bind ribosomes, and some can produce functional peptides (Chen et al, 2020 Science), and based on our results, different splice isoforms are bound by ribosomes in drug-resistant cells than in sensitive cells. This suggests that depending on the lncRNA splice isoform, the function of the lncRNA may be affected in drug-resistant cells. For example, *JPX*, a well-known nuclear lncRNAs, was found in the ribosomal RNA fractions, in our dataset as well as other datasets (Chen et al, 2020 Science), which indicates that some of its isoforms exist the nucleus. However, its function outside the nucleus remains unknown, and the question remains as to whether these lncRNAs produce functional peptides in the context of drug resistance. We also show that that alterations of lncRNAs with potential coding capacity correlate negatively with patient survival and positively with high PCa grade staging. These alterations generally correlated with the expression of these lncRNAs in patient samples (data not shown) suggesting that expression as well as alterations of these lncRNAs can serve as novel prognostic biomarkers for prostate cancer drug resistance. This, in turn, can lead to better targeted therapies.

In conclusion, our study highlights the importance of addressing the role of translation misregulation in PCa. Our model of PCa drug-resistance suggests that therapeutic targeting of translation factors and pathways should be revisited. We provide a comprehensive list of protein coding as well as lncRNA genes that can serve as markers for translation output in the context of PCa drug resistance. We demonstrate an unusual shift in ribosome binding from protein coding genes to lncRNAs, which clearly demonstrates a remodelling of the translatome of drug resistant cells. Is this remodeling a consequence or driver of drug resistance? Do these lncRNAs code for functional peptides or the fact that they bind to ribosomes lead to PCa drug resistance?

These questions remain to be answered; however, our study brings forward novel concepts and prognostic biomarkers that relate to the translation output of drug resistant cells.

METHODS

Cell culture and drugs

LNCaP and VCaP cell lines were from ATCC. All cell lines were cultivated at 37°C with 5% CO_2. LNCaP and MR49F (ENZ resistant derivated from LNCaP) were cultivated in RPMI 10% FBS whereas VCaP and $VCaP^{ER}$ (ENZ resistant derivated from VCaP) where cultivated in DMEM 10% FBS with 1mM sodium pyruvate. ENZ-resistant cell lines where maintained in 10 µM enzalutamide (ENZ).

Abiraterone, seviteronel (VT-464), enzalutamide (ENZ) and galeterone were kindly provided by Innocrin Pharmaceuticals Inc (Durham, NC). Metribolone (R1881) was purchased from Toronto Research Chemicals Inc (North York, ON).

Generation of enzalutamide-resistant cell lines in mice

All animal procedures were performed according to Canadian Council on Animal Care guidelines and with approval of the Animal Care Committee of the University of British Columbia (protocol # A12-0210). One million VCaP cells were inoculated on both flank of six-week-old male athymic nude mice (Harlan Sprague-Dawley, Inc). Two weeks later, mice were surgically castrated. Mice with castration-resistant tumor ($VCaP^{CRPC}$) were force-fed with 10mg/kg ENZ (or vehicle) 5 days per week until tumor recurrence ($VCaP^{ER}$). See Figure 1A.

LC-MS on mouse plasma

Immunofluorescence on cells for AR and AR-V7

VCaP and $VCaP^{ER}$ were plated on coverslip and treated with 10µM of abiraterone, VT-464, ENZ or galeterone with and without 0,1nM R1881 for 24h. Cells were then fixed with methanol. Non-specific binding sites were blocked in PBS containing 0.2% BSA and 0.1% Triton X100. Slides were incubated in primary and secondary antibodies diluted in blocking buffer for 1h. AR (Cell Signaling Technologie, Danvers, MA) and AR-V7antibodies (Santa Cruz Biotechnologies, Dallas, TX) were used 1/200. Secondary antibodies donkey anti-rabbit Alexa Fluor 488 (Invitrogen, Carlsbad, CA) and goat anti-mouse Alexa Fluor 594 (Abcam, Cambridge, UK) were diluted 1/1000. Nuclei were counterstained with Vectashield mounting

medium with DAPI (Vector Labs, Burlingame, CA). Images were acquired on Nikon Eclipse E600 epifluorescence microscope.

Immunofluorescence on mouse xenograft for CD68 and CD206

Frozen sections of mouse xenograft were first rehydrated in PBS and then blocked in PBS 10% FBS. They were incubated with primary antibodies against CD68 (1/800; Abcam) and CD206 (1/800; Abcam) in PBS 1% FBS for 1h. Fluorescent secondary antibodies were used as described previously. Slides were mounted in PBS:glycerol (1:1) with DAPI.

Western blot for AR and AR-V7

$VCaP^{CRPC}$ and $VCaP^{ER}$ cells were lysed in RIPA buffer containing protease and phosphatase inhibitors. Total proteins were separated by SDS-PAGE and transferred on nitrocellulose membrane. After blocking with 5% milk, membranes were blotted overnight with primary antibodies against AR, AR-V7 or β-actin as loading control (Cell signaling technologies) diluted 1/1000. Membranes were then incubated with HRP-conjugated secondary antibodies (Jackson ImmunoResearch Laboratories Inc, West Grove, PA) 2h in 5% milk (1/10 000). Proteins were imaged on Chemidoc MP (Bio-Rad, Hercules, CA) with ECL reagent.

Proliferation of ENZ resistance cell modal

Cell proliferation was measured using Cell-Counting Kit-8 (CCK8) (Dojindo, Gaithersburg, MD) which quantifies cellular dehydrogenase activity. Briefly, cells were seeded into 96-well plates and treated with 0.5 to 50 µM of ENZ. After 7 days, CCK-8 solution was added in media for a final concentration of 10% and incubated at 37°C for 3h. Cell growth was determined by optical density (OD) measurements at 450 nm with TECAN Infinite F50. Calculations were performed according to manufacturer's instructions. Experiment was repeated 3 times with each cell line.

Polysomal profiles and analysis of polysomal-associated RNAs

$VCaP^{CRPC}$, $VCaP^{ER}$, LNCaP and MR49F cells were grown in 100-mm tissue culturue dishes to ~ 80% confluence. Only $VCaP^{ER}$ and MR49F were treated with ENZ at 10 µM. Cells were scrapped in 1 mL of polysomal buffer (20 mM Tris, pH 7.5, 150 mM NaCl, 1.25 mM $MgCl_2$, 5 U/mL RNAsine, EDTA-free inhibitor cocktail [Complete; Roche, Indianapolis, IN a verifier], and 1 mM dithiothreitol), and Nonidet P-40 was added to a final concentration of 1% for lysis of 15 min on ice. Extracts were clarified by centrifugation at 12,000 g for 20 min at 4°C. After measure the concentration of RNAs present using a spectrophotometer, ~20 OD_{260} units was

loaded onto the 15-55% sucrose gradient. The gradients were centrifuged for 2 hr 30 at 37,000 rpm. Then, sucrose gradients were placed on Automated Density Fractionation System and proceed with automated fractionation and collection of fractions. Each fraction has been collected into individual tubes with continuous monitoring of absorbance at 254 nm. The polyribosomal profile was editing on the chart paper. At the end each fraction has follow RNA extraction and send to RNA-Sequencing.

cDNA library construction and sequencing

Total RNA was extracted with the Trizol reagent (Life Technology° and polyribosomal RNA was prepared by phenol-chloroform extraction.

Analysis of differentially expressed genes or associated RNA to ribosomes

Sample preparation for Mass Spectrometry

Protein pellets were resuspended in 100 µL of 50 mM ammonium bicarbonate, 0.5% deoxycholate and sonicated on ice with a microprobe Sonic Dismembrator 550 (Fisher Scientific) as follow: 20 x 1 seconds at power 2 followed by 5 x 3 seconds at power 4. The extract was centrifuged at 20,817 g for 15 minutes at 4°C. The supernatants were transferred to new tubes and precipitated with acetone. The protein pellets were then resuspended in 100 µL of 500mM triethylammonium bicarbonate, 0.5% deoxycholate. Protein concentrations of each sample was determined by colorimetric Bradford assay.

Tryptic digestion and TMT labeling

10µg of each sample was used for TMT labeling (Thermo Fisher Scientific). Proteins were denatured for 5 minutes at 95°C and then reduced with 50mM TCEP for 30 minutes at 37°C before being alkylated with 100mM iodoacetamide for 30 minutess at room temperature in the dark. Samples were digested with 0.5 µg of trypsin (V5111; Promega) for ~15 hours at 37°C. After digestion, peptides were acidified to precipitate the deoxycholate and then purified with homemade C18 Stage-Tip before being lyophilized. The now dried peptides were dissolved in 30 µL of 100 mM triethylammonium bicarbonate and labeled with TMT 10-plex reagent (Thermo Fischer Scientific). Labeling was performed for 1 hour at room temperature and the reaction quenched with hydroxylamine for 15 minutes. The now labeled peptides were combined in one tube and speedvac to dryness without heat. Samples were cleaned up using solid-phase HLB cartridge (Water Corp.) before being speedvac to dryness.

High pH - reverse phase fractionation

Peptides were fractionated into 14 fractions using a High-pH (pH 10) reversed-phase chromatography method using an Agilent 1200 HPLC system as previously described (PMID: 21500348). The final fractions were dried and resuspended in 0.1% formic acid before mass spectrometry analysis.

Mass spectrometry analysis

Approximately 1 µg of each fraction was injected and separated by online reversed-phase (RP) nanoscale capillary liquid chromatography (nanoLC) and analyzed by electrospray mass spectrometry (ESI MS/MS). The experiments were performed with a Dionex UltiMate 3000 nanoRSLC chromatography system (Thermo Fisher Scientific / Dionex Softron GmbH, Germering, Germany) coupled to an Orbitrap Fusion mass spectrometer (Thermo Fisher Scientific, San Jose, CA, USA) equipped with a nanoelectrospray ion source. Peptides were trapped at 20 µl/min in loading solvent (2% acetonitrile, 0.05% TFA) on a 5 mm x 300 µm C18 PepMap cartridge pre-column (Thermo Fisher Scientific / Dionex Softron GmbH, Germering, Germany) for 5 minutes. Then, the pre-column was switched online with a 75 µm x 50 cm Acclaim PepMap100 C18-3µm column (Thermo Fischer Scientific/ Dionex Softron GmbH, Germering, Germany) and the peptides were eluted with a linear gradient from 5-40% solvent B (A: 0,1% formic acid, B: 80% acetonitrile, 0.1% formic acid) in 90 minutes at 300 nL/min. Mass spectra were acquired using a data dependent acquisition mode using Thermo XCalibur software version 3.0.63. Synchronous Precursor Selection-MS3 acquisition mode was used for this analysis. Full scan mass spectra (380 to 1500m/z) were acquired in the Orbitrap at a 60 000 resolution and using an AGC target of 2e5, a maximum injection time of 50m. Internal calibration, using lock mass on the m/z 445.12003 siloxane ion, was used. Precursors for MS2/MS3 analysis were selected using a TopSpeed of 3s. The most intense precusor ions were isolated in the quadrupole at 0.7m/z, fragmented with 35% CID and the fragments detected in the ion trap. Following acquisition of each MS2 spectrum, an MS3 acquisition was performed by isolating of multiple MS2 fragment ions with a multi-notch isolation waveform (PMID: 24927332). MS3 analysis was detected in the Orbitrap at a 60 000 resolution after 45% HCD, with an AGC target of 1e5 and a maximum injection time of 120 ms. Dynamic exclusion of previously fragmented peptides was set for a period of 20 seconds and a tolerance of 10 ppm.

Data analysis

Spectra acquired were processed using ProteomeDiscoverer 2.2 (Thermo). Files were search against Uniprot[49] homo sapiens protein database (93634 entries). Trypsin was set as enzyme and 2 missed cleavages were allowed. Deamidation (N, Q), oxidation (M), were set as dynamic modifications and carbamidomethylation (C), and TMT10-plex label (N-ter, K) were set as static modifications. Mass search tolerance were 10 ppm and 0.6 Da for MS and MS/MS respectively. For protein validation, a maximum False Discovery Rate of 1% at peptide and protein level was used based on a target/decoy search. MS3 spectra were used for quantification, with an integration tolerance of 10 ppm. Unique and razor peptides are considered for protein quantification and isotopic correction is applied on reporters. Data normalisation was performed on total peptide amount. Peptides and protein result tabs were exported in Excel. Mean of three replicates by groups are calculated and a protein or a peptide is considered as up-regulated if its z-score > 1.96 and p-value < 0.05 and down-regulated if its z-score < -1.96 and p-value < 0.05.

Analysis of differentially expressed genes and RNAs bound to ribomes

Western blot

$VCaP^{CRPC}$ and $VCaP^{ER}$ cells were lysed in RIPA buffer containing protease and phosphatase inhibitors. Total proteins were separated by SDS-PAGE and transferred on PVDF membrane. After blocking with 5% milk or 5% BSA, membranes were blotted overnight with primary antibodies against NUDT19 or alpha-tubulin as loading control diluted respectively in 1/10000 and 1/20000. Membranes were then incubated with HRP-conjugated secondary antibodies 2h in 5% milk (1/10 000). Proteins were imaged by scanner with ECL reagent.

PCa patient cohort

This study was approved by the research ethics committee of CHU de Québec-Université Laval (Project 2016-2811). A sub-cohort of the CPC-GENE cohort (PMID: 28068672) was used for this study. The cohort comprised 136 men with intermediate risk PCa who underwent radical prostatectomy between 2005 and 2010 at CHU de Québec-Université Laval. Complete clinico-pathological data were available for all 136 subjects with a median follow-up of 11.8 years. Archived formalin-fixed and paraffin embedded specimens of radical prostatectomy from the 136 subjects were used to construct a tissue microarray (TMA).

Immunohistochemistry on prostate tumor microarray (TMA)

Four micrometer-thick sections of the TMA blocks were first deparaffinized and rehydrated. Antigen unmasking was carried out in a DAKO PT-Link for 20 minutes at 97°C using EnVision FLEX buffer of appropriate pH for each antibody (Agilent, Santa Clara, CA). Then, peroxidases were inactivated in a 3% hydrogen peroxide solution. After incubation with a blocking solution, slides were stained overnight with antibodies against Acyl-CoA Synthetase Long Chain Family Member 5 (ACSL5; 50µg/mL; Sigma-Aldrich, Oakville, ON), Enoyl-CoA Hydratase Domain Containing 3 (ECHDC3; 0.5µg/mL; Invitrogen) and Nudix Hydrolase 19 (NUDT19; 3.3µg/mL; Abcam) diluted in PBS containing 1% BSA. After washed, staining was revealed using the IDetect Super strain HRP polymer kit (Agilent) following manufacturer's protocol. After DAB revelation, slides were counterstained with hematoxylin.

For each target, tissue samples were classified according to tumor staining intensity from 1 to 3. Intensity variation was also considered. Result for each patient is a mean of 3 cores. Results were confirmed by a second reader.

DATA ACCESS

ACKNOWLEDGMENTS

Authors contributions

DISCLOSURE DECLARATION

REFERENCES

1. Gebauer, F. & Hentze, M. W. Molecular mechanisms of translational control. *Nat Rev Mol Cell Bio* **5**, 827–835 (2004).

2. Holcik, M. & Sonenberg, N. Translational control in stress and apoptosis. *Nat Rev Mol Cell Bio* **6**, 318–327 (2005).

3. Hershey, J. W. B., Sonenberg, N. & Mathews, M. B. Principles of Translational Control. *Csh Perspect Biol* **11**, a032607 (2019).

4. Panniers, R. Translational control during heat shock. *Biochimie* **76**, 737–747 (1994).

5. Richter, K., Haslbeck, M. & Buchner, J. The Heat Shock Response: Life on the Verge of Death. *Mol Cell* **40**, 253–266 (2010).

6. Miluzio, A. *et al.* Impairment of cytoplasmic eIF6 activity restricts lymphomagenesis and tumor progression without affecting normal growth. *Cancer Cell* **19**, 765–75 (2011).

7. Barna, M. *et al.* Suppression of Myc oncogenic activity by ribosomal protein haploinsufficiency. *Nature* **456**, 971–5 (2008).

8. Furic, L. *et al.* eIF4E phosphorylation promotes tumorigenesis and is associated with prostate cancer progression. *P Natl Acad Sci Usa* **107**, 14134–9 (2010).

9. Hsieh, A. C. *et al.* Genetic dissection of the oncogenic mTOR pathway reveals druggable addiction to translational control via 4EBP-eIF4E. *Cancer Cell* **17**, 249–61 (2010).

10. Faller, W. J. *et al.* mTORC1-mediated translational elongation limits intestinal tumour initiation and growth. *Nature* **517**, 497–500 (2014).

11. Truitt, M. L. *et al.* Differential Requirements for eIF4E Dose in Normal Development and Cancer. *Cell* **162**, 59–71 (2015).

12. Pedersen, M. T. & Jensen, K. B. Unconventional translation in cancer. *Nature* **541**, 471–472 (2017).

13. Lockshin, R. A. & Zakeri, Z. Cell death in health and disease. *J Cell Mol Med* **11**, 1214–1224 (2007).

14. Nguyen, H. G. *et al.* Development of a stress response therapy targeting aggressive prostate cancer. *Sci Transl Med* **10**, eaar2036 (2018).

15. Biffo, S., Manfrini, N. & Ricciardi, S. Crosstalks between translation and metabolism in cancer. *Curr Opin Genet Dev* **48**, 75–81 (2018).

16. Patra, K. C. & Hay, N. The pentose phosphate pathway and cancer. *Trends Biochem Sci* **39**, 347–54 (2014).

17. Swinnen, J. V., Brusselmans, K. & Verhoeven, G. Increased lipogenesis in cancer cells: new players, novel targets. *Curr Opin Clin Nutr* **9**, 358–365 (2006).

18. Santos, C. R. & Schulze, A. Lipid metabolism in cancer. *Febs J* **279**, 2610–23 (2012).

19. Kim, J., Tchernyshyov, I., Semenza, G. L. & Dang, C. V. HIF-1-mediated expression of pyruvate dehydrogenase kinase: A metabolic switch required for cellular adaptation to hypoxia. *Cell Metab* **3**, 177–185 (2006).

20. Pavlova, N. N. & Thompson, C. B. The Emerging Hallmarks of Cancer Metabolism. *Cell Metab* **23**, 27–47 (2016).

21. Heiden, M. G. V. & DeBerardinis, R. J. Understanding the Intersections between Metabolism and Cancer Biology. *Cell* **168**, 657–669 (2017).

22. Xiong, Y. *et al.* Flexibility in metabolism bestows tenacious viability on cancer. *Life Sci* **208**, 20–25 (2018).

23. Bhat, M. *et al.* Targeting the translation machinery in cancer. *Nat Rev Drug Discov* **14**, 261–78 (2015).

24. Karaki, S., Andrieu, C., Ziouziou, H. & Rocchi, P. The Eukaryotic Translation Initiation Factor 4E (eIF4E) as a Therapeutic Target for Cancer. *Adv Protein Chem Str* **101**, 1–26 (2015).

25. Kuersten, S., Radek, A., Vogel, C. & Penalva, L. O. F. Translation regulation gets its 'omics' moment. *Wiley Interdiscip Rev Rna* **4**, 617–630 (2013).

26. Vickers, A. J., Savage, C., O'Brien, M. F. & Lilja, H. Systematic review of pretreatment prostate-specific antigen velocity and doubling time as predictors for prostate cancer. *J Clin Oncol Official J Am Soc Clin Oncol* **27**, 398–403 (2008).

27. Boorjian, S. A. *et al.* A Critical Analysis of the Long-Term Impact of Radical Prostatectomy on Cancer Control and Function Outcomes. *Eur Urol* **61**, 664–675 (2012).

28. KRYGIEL, J. M. *et al.* INTERMEDIATE TERM BIOCHEMICAL PROGRESSION RATES AFTER RADICAL PROSTATECTOMY AND RADIOTHERAPY IN PATIENTS WITH SCREEN DETECTED PROSTATE CANCER. *J Urology* **174**, 126–130 (2005).

29. Liu, Y. *et al.* The androgen receptor regulates a druggable translational regulon in advanced prostate cancer. *Sci Transl Med* **11**, eaaw4993 (2019).

30. Kuruma, H. *et al.* A Novel Antiandrogen, Compound 30, Suppresses Castration-Resistant and MDV3100-Resistant Prostate Cancer Growth In Vitro and In Vivo. *Mol Cancer Ther* **12**, 567–576 (2013).

31. Geller, J., Albert, J., Nachtsheim, D., Loza, D. & Lippman, S. Steroid levels in cancer of the prostate--markers of tumor differentiation and adequacy of anti-androgen therapy. *Prog Clin Biol Res* **33**, 103–11 (1979).

32. Mohler, J. L. *et al.* The Androgen Axis in Recurrent Prostate Cancer. *Clin Cancer Res* **10**, 440–448 (2004).

33. CPTAC, N. *et al.* Proteogenomics connects somatic mutations to signalling in breast cancer. *Nature* **534**, 55–62 (2016).

34. Zhang, B. *et al.* Proteogenomic characterization of human colon and rectal cancer. *Nature* **513**, 382–387 (2014).

35. Woo, Y. H. & Li, W.-H. Evolutionary Conservation of Histone Modifications in Mammals. *Mol Biol Evol* **29**, 1757–1767 (2012).

36. Jiao, X. *et al.* DAVID-WS: a stateful web service to facilitate gene/protein list analysis. *Bioinformatics* **28**, 1805–1806 (2012).

37. Doncheva, N. T., Morris, J. H., Gorodkin, J. & Jensen, L. J. Cytoscape StringApp: Network Analysis and Visualization of Proteomics Data. *J Proteome Res* **18**, 623–632 (2018).

38. Cerami, E. *et al.* The cBio Cancer Genomics Portal: An Open Platform for Exploring Multidimensional Cancer Genomics Data. *Cancer Discov* **2**, 401–404 (2012).

39. Gao, J. *et al.* Integrative Analysis of Complex Cancer Genomics and Clinical Profiles Using the cBioPortal. *Sci Signal* **6**, pl1–pl1 (2013).

40. Nadiminty, N. *et al.* NF-κB2/p52 Induces Resistance to Enzalutamide in Prostate Cancer: Role of Androgen Receptor and Its Variants. *Mol Cancer Ther* **12**, 1629–1637 (2013).

41. Mostaghel, E. A. *et al.* Resistance to CYP17A1 Inhibition with Abiraterone in Castration-Resistant Prostate Cancer: Induction of Steroidogenesis and Androgen Receptor Splice Variants. *Clin Cancer Res* **17**, 5913–5925 (2011).

42. Hua, H. *et al.* Targeting mTOR for cancer therapy. *J Hematol Oncol* **12**, 71 (2019).

43. Hsu, C.-C., Tseng, L.-M. & Lee, H.-C. Role of mitochondrial dysfunction in cancer progression. *Exp Biol Med* **241**, 1281–1295 (2016).

44. Yang, Y. *et al.* Mitochondria and Mitochondrial ROS in Cancer: Novel Targets for Anticancer Therapy. *J Cell Physiol* **231**, 2570–2581 (2016).

45. Kim, H.-J., Maiti, P. & Barrientos, A. Mitochondrial ribosomes in cancer. *Semin Cancer Biol* **47**, 67–81 (2017).

46. D'Souza, A. R. & Minczuk, M. Mitochondrial transcription and translation: overview. *Essays Biochem* **62**, 309–320 (2018).

47. Ren, K. *et al.* The over-expression of Pim-2 promote the tumorigenesis of prostatic carcinoma through phosphorylating eIF4B. *Prostate* **73**, 1462–1469 (2013).

48. Guo, X. *et al.* Human ribosomal protein S13 promotes gastric cancer growth through down-regulating p27Kip1. *J Cell Mol Med* **15**, 296–306 (2011).

49. The UniProt Consortium. UniProt: the universal protein knowledgebase. *Nucleic Acids Res* **45**, D158–D169 (2017).

FIGURE LEGENDS

Figure 1. Establishment of Enzalutamide (ENZ)-resistant Prostate Cancer (PCa) cellular models. (A) Experimental approach used to establish PCa resistance acquisition in mice models, as well as the derivation of ENZ-sensitive and ENZ-resistant cell lines in culture: One million cells from an ENZ-sensitive prostate cell line called VCaP were inoculated in athymic nude male mice. The mice were then surgically castrated (Cx), leading to development of castration-resistant PCa (CRPC) cells. The latter were extracted from the tumors to establish the $VCaP^{CRPC}$ cell line. Finally, mice resistant to castration were treated with 10 µM ENZ (Tx) until tumor recurrence. ENZ-resistant cells were extracted from those to establish the $VCaP^{ER}$ cell line and maintained under the same conditions. **(B)** Cell proliferation assays on $VCaP^{CRPC}$ and $VCaP^{ER}$ cell lines performed in the absence or presence of increasing quantities of ENZ confirms that ENZ treatment only affects proliferation of sensitive $VCaP^{CRPC}$ cells. **(C)** Western-Blot reveals a higher expression of the Androgen Receptor (AR) in $VCaP^{ER}$ compared to $VCaP^{CRPC}$ cells, as well as a specific expression of the AR splice variant AR-V7 in the ENZ-resistant $VCaP^{ER}$ cell line. **(D)** Experimental pipeline used to analyze the transcriptome (*i.e.* total RNAs), translatome (*i.e.* ribosome-bound RNAs) and proteome (*i.e.* total proteins) from the different cell lines: Total RNAs from VCaP, $VCaP^{CRPC}$ and $VCaP^{ER}$ cells were extracted and submitted to RNA sequencing. Polysome profiling from both $VCaP^{CRPC}$ and $VCaP^{ER}$ cells was performed on soluble RNAs to isolate heavy polysome fractions from which RNAs were subsequently sequenced. Finally, total proteins from all cell lines were analyzed by mass spectrometry. **(E)** Pearson correlation shows both a high correlation between the transcriptome and proteome (empty dots) and between the translatome and proteome (full dots) of the $VCaP^{CRPC}$ cell line. **(F)** Pearson correlation highlights a high correlation between the transcriptome and proteome (empty circles) but a slightly lower correlation between the translatome and proteome (full circles) of the $VCaP^{ER}$ cells.

Figure 2. GO-term enrichment analysis of differentially expressed genes and genes differentially associated to ribosomes reveals differentially enriched terms in $VCaP^{ER}$ and $VCaP^{CRPC}$ cell lines. (A) Dot plot and **(B)** Venn diagram quantification highlighting the RNAs that are significantly expressed (empty circles) or bound to ribosomes (full circles) in $VCaP^{ER}$ (red) compared to $VCaP^{CRPC}$ (blue) cells. Genes in colour have an adjusted P value <0.05 (n=3 per group for polysome profiling; n=2 for RNA sequencing). **(C)** GO term enrichment analysis with DAVID 6.8 shows terms for cellular components (GOCC) enriched for the genes

upregulated in the translatome or transcriptome of VCaP^{ER} (red) or VCaP^{CRPC} (blue) cell lines. **(D)** Gene set enrichment analysis (GSEA) results from total RNAs and RNAs from polysome sequencing shows the enrichment scores (ES) in biological pathways upregulated in VCaP^{ER} (red) or VCaP^{CRPC} (blue).

Figure 3. Changes occur in the proteomic landscape during resistance acquisition. (A) Mass spectrometry results shows hundreds of proteins differentially expressed in VCaP^{ER} cells in comparison to VCaP^{CRPC} and VCaP cell lines. **(B)** GO term enrichment analysis with DAVID 6.8 shows terms for biological processes (GOBP) and cellular components (GOCC) enriched for genes which proteins were down- (blue) or up-regulated (red) in VCaP^{ER} cell line. Network analysis using stringApp on Cytoscape shows clusters formed by proteins **(C)** upregulated or **(D)** downregulated in VCaP^{ER} cell line. These interactions include interactions predicted by curated databases. **(E)** Kaplan-Meier graph of disease-free survival for patients with or without alterations in genes coding for proteins up- or **(F)** downregulated in VCaP^{ER}. We found that alterations in genes coding for identified DEPs in VCaP^{ER} corresponded to significantly lower disease-free survival over time in PCa patients.

Figure 4. Enzalutamide resistance induces shifts in translation efficiency. (A) Volcano plot shows genes with high (red) and low (blue) translation efficiencies differentially expressed in VCaP^{ER} compared to VCaP^{CRPC}. Genes with high or low TEs in VCaP^{ER} are highlighted. Upregulated proteins with high translation efficiency (TE) and downregulated proteins with low TE are marked in cyan and purple respectively. **(B)** GO term enrichment analysis with DAVID 6.8 shows terms for cellular components (GOCC) enriched in genes with low (blue) or high (red) TEs in VCaP^{ER} compared to VCaP^{CRPC}. **(C)** Differential TE (DTE) in VCaP^{ER} compared to VCaP^{CRPC}. **(D)** Kaplan-Meier graph of overall survival for PCa patients with or without alterations in genes with either high or **(E)** low TE ratios. **(F)** Percentages of BioChemical Recurrence (BCR) for patients expressing high, medium or low levels of NUDT19, calculated from immunohistochemistry on PCa microarray. **(G)** Scatter plots for differential expression bins for NUTD19 and AR (high) or ARV7 (bottom).

Figure 5. Aberrant association of lncRNAs to ribosomes may play a role in cancer resistance. (A) TE ratio distributions of all genes or genes with differential translation efficiency (DTE) in VCaP^{ER} vs VCaP^{crpc} for mRNAs and lncRNAs. **(B)** Volcano plot shows potentially coding lncRNAs with high (red) and low (blue) translation efficiencies differentially

expressed in VCaP^{ER} compared to VCaP^{CRPC}. **(C)** Kaplan-Meier graph of overall survival for PCa patients with or without alterations in lncRNAs with high TE ratios. **(D)** Quantification of lncRNAs having a positive or negative impact on survival for candidates with either high or low TE ratios. **(E)** Distribution of Gleason scores for patients with or without alterations in genes with high or low TE ratio is not significantly different. **(F)** Sashimi plots in PCa resistant cell lines show alternative splicing of *JPX* (left) or *LINC00467* (right) lncRNAs with high TE levels which alterations have an effect on patient survival is affected in VCaP^{ER}. **(G)** Quantification of *JPX* or **(H)** *LINC00467* lncRNA read counts in the transcriptome and translatome of VCaP^{CRPC} (blue) or VCaP^{ER} cell lines.

Figure S1: Polysome profiling on ENZ-sensitive and -resistant cell lines show similar patterns. Polysome profiling experiments performed in ENZ-sensitive **(A)** VCaP^{CRPC} and **(C)** LNCaP or ENZ-resistant **(B)** VCaP^{ER} and **(D)** MR49F cell lines, with resistant cell lines cultured in 10 μM ENZ. Peaks show ribosomal subunits (40S and 60S), mono-ribosomes (M), light (LP) and heavy polysomes (HP), distributed along a sucrose sedimentation gradient. Total mRNA level is positively correlated with RNA association to ribosomes (p-value < 0.0001, Pearson correlation) both in **(E)** VCaP^{CRPC} and **(F)** VCaP^{ER} cell lines. Pearson correlation coefficients (ρ) and linear regression (grey lines) are indicated. ENZ: Enzalutamide, CRPC: Castration-Resistant Prostate Cancer, ER: Enzalutamide-Resistant.

Figure S2: GO-term enrichment analysis and GSEA of transcriptomes and translatomes for VCaP^{ER} and VCaP^{CRPC} show significantly enriched gene sets. (A) GO-term enrichment analysis with DAVID 6.8 shows terms for biological processes (GOBP) and molecular functions (GOMF) enriched in either VCaP^{ER} or VCaP^{CRPC}. **(B)** Gene set enrichment analysis (GSEA) enrichment scores (ES) for significantly enriched GO-terms in either VCaP^{ER} (red) or VCaP^{CRPC} (blue) transcriptomes and translatomes. Spearman correlation of enrichment scores shows a slightly higher correlation coefficient between transcriptome and translatome in VCaP^{ER}, when compared to VCaP^{CRPC}. Selected GO-terms are highlighted. Enrichment plots for selected GO-terms for **(C)** VCaP^{ER} polysomes, **(D)** VCaP^{CRPC} polysomes **(E)** VCaP^{ER} total RNA and **(F)** VCaP^{CRPC} total RNA.

Figure S3: Pearson correlation reveals strong correlation between MR49F proteome and VCaP^{ER} proteome. (A) GO-term enrichment analysis shows terms for molecular functions

(GOMF) and Kyoto Encyclopedia of Genes and Genomes (KEGG) pathways enriched in the proteins either upregulated or downregulated in VCaP^{ER} cell line in comparison to VCaP^{CRPC}. **(B)** Spearman correlation of protein abundances between MR49F and VCaP^{ER} or **(C)** VCaP^{CRPC}. Density plots show MR49F expression of proteins **(B)** up- or **(C)** downregulated in VCaP^{ER}. **(D)** Kaplan-Meier graph of cancer progression-free survival for patients with or without alterations in genes coding for proteins up- or **(E)** downregulated in VCaP^{ER}.

Figure S4: Progression free survival of PCa patients shows a better outcome for patients with genomic alterations in genes upregulated in VCap^{ER} cells. (A) Volcano plot shows proteins detected by Mass Spectrometry (MS) differentially expressed between VCaP^{ER} and VCaP^{CRPC}. Proteins up- or downregulated in VCaP^{ER} are highlighted. Upregulated proteins with high translation efficiency (TE) and downregulated proteins with low TE are marked in cyan and purple respectively. **(B)** Protein expression of NUDT19 in VCaP^{ER}, VCaP^{CRPC}, LNCaP and MR49F, shown in triplicate lanes. **(C)** Quantification of the protein levels of NUDT19 in VCaP^{ER} or MR49F cell lines respectively normalized to VCaP^{CRPC} or LNCaP.

Figure S5: Genes with high TE ratios are enriched in specific gene ontology terms, but their alteration is not linked to higher cancer grade in patients. (A) GO term enrichment analysis with DAVID 6.8 shows terms for biological processes (GOBP) and molecular functions (GOMF) enriched in genes with low or high TEs in VCaP^{ER} compared to VCaP^{CRPC}. **(B)** Distribution of Gleason scores for patients with or without alterations in genes with high or **(C)** low TE ratio is not significantly different.

Figure S6: (A) Observed vs. expected gene counts of different categories of genes from both the translatome and transcriptome in VCaP^{ER} compared to VCaP^{CRPC}. Significant enrichment in VCaP^{ER} compared to VCaP^{CRPC} (p-value < 0.05) is only observed for long non-coding RNAs (lncRNAs) and processed transcripts. **(B)** Observed vs. expected gene counts of coding vs. non-coding genes with high translation efficiencies in VCaP^{ER} compared to VCaP^{CRPC}. **(C)** Kaplan-Meier graph of overall survival for PCa patients with or without alterations in lncRNAs with wither high (left) or low (right) TE ratios. **(D)** Kaplan-Meier graph of overall survival for PCa patients with alterations in single lncRNAs with low TE ratios. **(E)** Sashimi plots in PCa resistant cell lines show alternative splicing of a lncRNA with a high TE level which alteration have an effect on patient survival (*WARS2-AS1*) is affected in VCaP^{ER}.

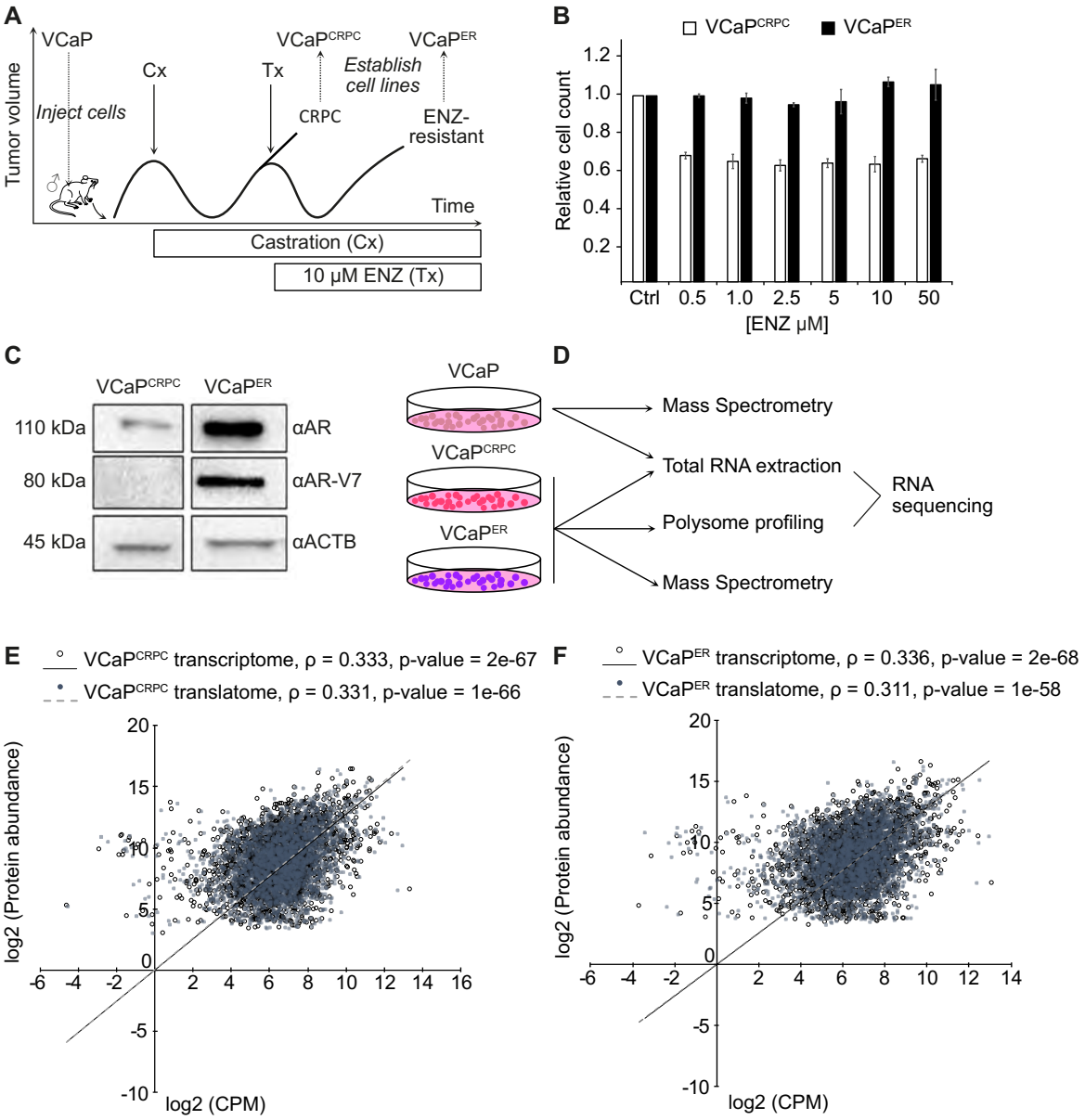
A
VCaP
Tumor volume
Inject cells
Cx
Tx
VCaP^CRPC
VCaP^ER
Establish cell lines
CRPC
ENZ-resistant
Time
Castration (Cx)
10 μM ENZ (Tx)
B
VCaP^CRPC
VCaP^ER
Relative cell count
1.2
1.0
0.8
0.6
0.4
0.2
Ctrl
0.5
1.0
2.5
5
10
50
[ENZ μM]
C
VCaP^CRPC
VCaP^ER
110 kDa
80 kDa
45 kDa
αAR
αAR-V7
αACTB
D
VCaP
VCaP^CRPC
VCaP^ER
Mass Spectrometry
Total RNA extraction
Polysome profiling
Mass Spectrometry
RNA sequencing
E
VCaP^CRPC transcriptome, ρ = 0.333, p-value = 2e-67
VCaP^CRPC translatome, ρ = 0.331, p-value = 1e-66
log2 (Protein abundance)
log2 (CPM)
F
VCaP^ER transcriptome, ρ = 0.336, p-value = 2e-68
VCaP^ER translatome, ρ = 0.311, p-value = 1e-58
log2 (Protein abundance)
log2 (CPM)

Figure 1

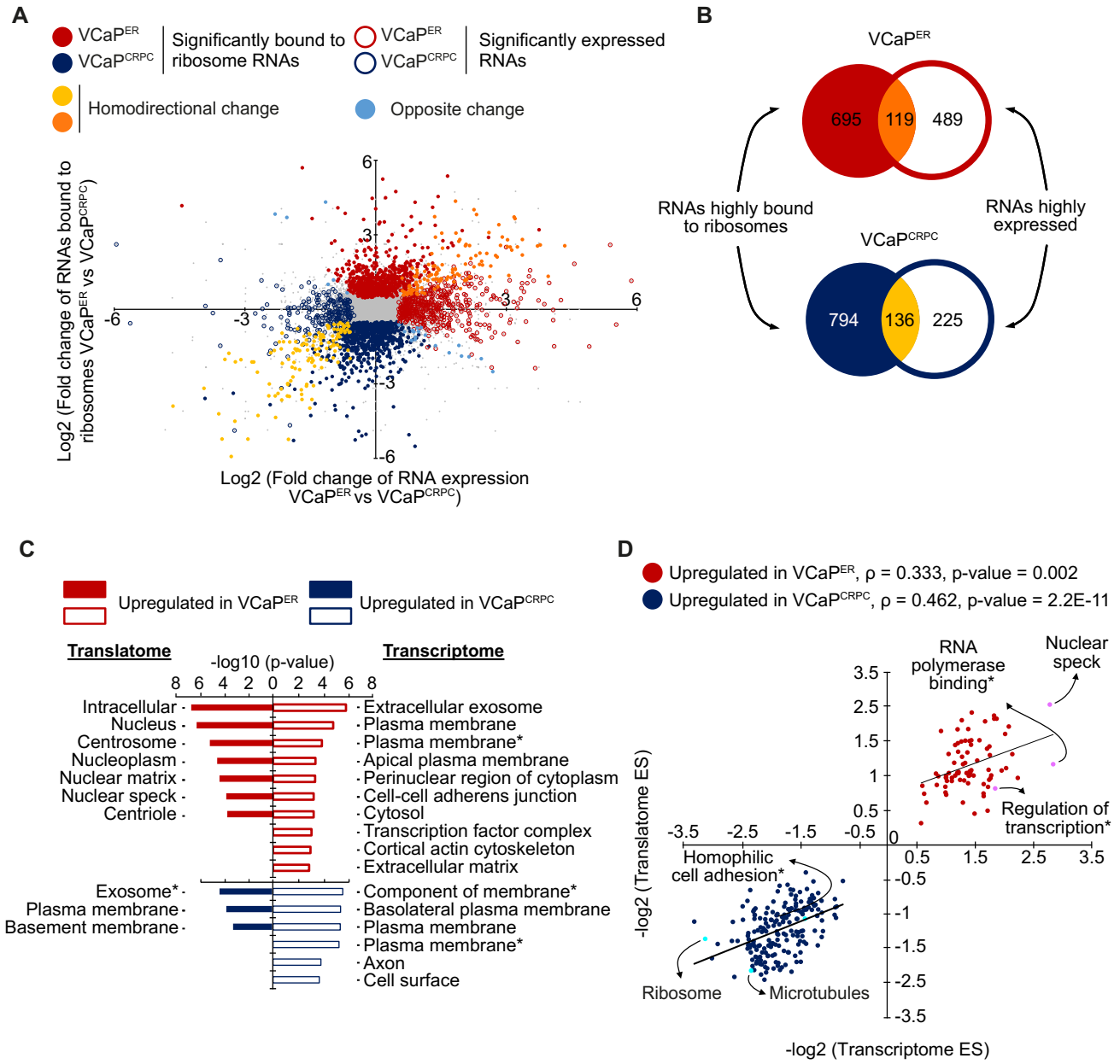
A
VCaP^ER
VCaP^CRPC
Significantly bound to ribosome RNAs
VCaP^ER
VCaP^CRPC
Significantly expressed RNAs
Homodirectional change
Opposite change
Log2 (Fold change of RNAs bound to ribosomes VCaP^ER vs VCaP^CRPC)
Log2 (Fold change of RNA expression VCaP^ER vs VCaP^CRPC)
B
VCaP^ER
695
119
489
RNAs highly bound to ribosomes
RNAs highly expressed
VCaP^CRPC
794
136
225
C
Upregulated in VCaP^ER
Upregulated in VCaP^CRPC
Translatome
-log10 (p-value)
Transcriptome
Intracellular
Nucleus
Centrosome
Nucleoplasm
Nuclear matrix
Nuclear speck
Centriole
Extracellular exosome
Plasma membrane
Plasma membrane*
Apical plasma membrane
Perinuclear region of cytoplasm
Cell-cell adherens junction
Cytosol
Transcription factor complex
Cortical actin cytoskeleton
Extracellular matrix
Exosome*
Plasma membrane
Basement membrane
Component of membrane*
Basolateral plasma membrane
Plasma membrane
Plasma membrane*
Axon
Cell surface
D
Upregulated in VCaP^ER, ρ = 0.333, p-value = 0.002
Upregulated in VCaP^CRPC, ρ = 0.462, p-value = 2.2E-11
RNA polymerase binding*
Nuclear speck
Regulation of transcription*
Homophilic cell adhesion*
Ribosome
Microtubules
-log2 (Translatome ES)
-log2 (Transcriptome ES)

Figure 2

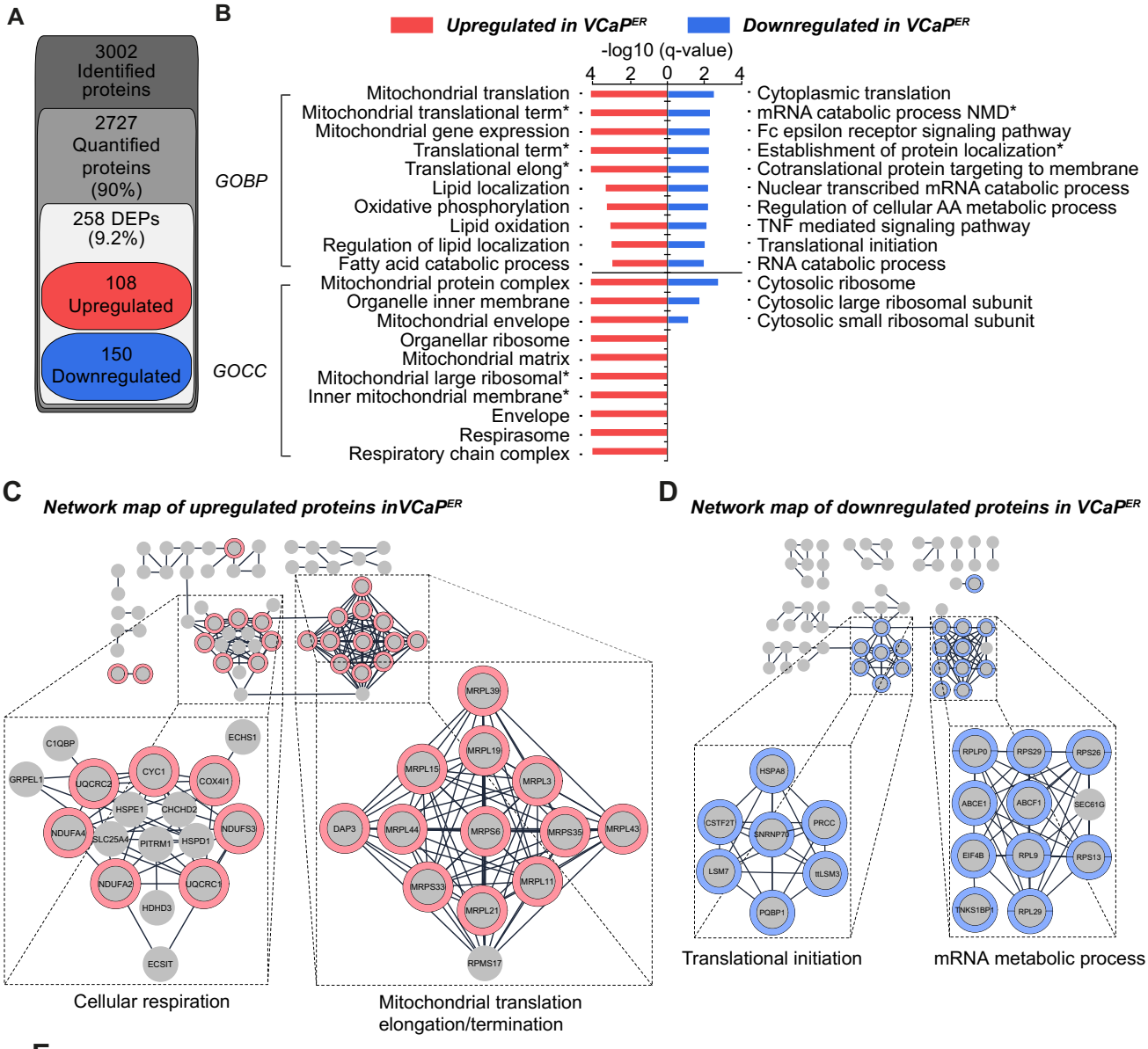
A
3002 Identified proteins
2727 Quantified proteins (90%)
258 DEPs (9.2%)
108 Upregulated
150 Downregulated
B
Upregulated in VCaP^ER
Downregulated in VCaP^ER
-log10 (q-value)
4 2 0 2 4
GOBP
Mitochondrial translation
Mitochondrial translational term*
Mitochondrial gene expression
Translational term*
Translational elong*
Lipid localization
Oxidative phosphorylation
Lipid oxidation
Regulation of lipid localization
Fatty acid catabolic process
GOCC
Mitochondrial protein complex
Organelle inner membrane
Mitochondrial envelope
Organellar ribosome
Mitochondrial matrix
Mitochondrial large ribosomal*
Inner mitochondrial membrane*
Envelope
Respirasome
Respiratory chain complex
Cytoplasmic translation
mRNA catabolic process NMD*
Fc epsilon receptor signaling pathway
Establishment of protein localization*
Cotranslational protein targeting to membrane
Nuclear transcribed mRNA catabolic process
Regulation of cellular AA metabolic process
TNF mediated signaling pathway
Translational initiation
RNA catabolic process
Cytosolic ribosome
Cytosolic large ribosomal subunit
Cytosolic small ribosomal subunit
C
Network map of upregulated proteins inVCaP^ER
C1QBP
ECHS1
GRPEL1
UQCRC2
CYC1
COX4I1
HSPE1
CHCHD2
NDUFA4
SLC25A4
PITRM1
HSPD1
NDUFS3
NDUFA2
UQCRC1
HDHD3
ECSIT
MRPL39
MRPL19
MRPL15
MRPL3
DAP3
MRPL44
MRPS6
MRPS35
MRPL43
MRPS33
MRPL11
MRPL21
RPMS17
Cellular respiration
Mitochondrial translation elongation/termination
D
Network map of downregulated proteins in VCaP^ER
HSPA8
CSTF2T
SNRNP70
PRCC
LSM7
tILSM3
PQBP1
RPLP0
RPS29
RPS26
ABCE1
ABCF1
SEC61G
EIF4B
RPL9
RPS13
TNKS1BP1
RPL29
Translational initiation
mRNA metabolic process
E
Upregulated proteins
Unaltered group
Altered group
q-value = 1.648e-3
100%
80%
60%
40%
20%
0%
Disease Free
0 20 40 60 80 100 120 140 160
Disease Free (Months)
F
Downregulated proteins
Unaltered group
Altered group
q-value = 0.0332
100%
80%
60%
40%
20%
0%
Disease Free
20 40 60 80 100 120 140 160
Disease Free (Months)

Figure 3

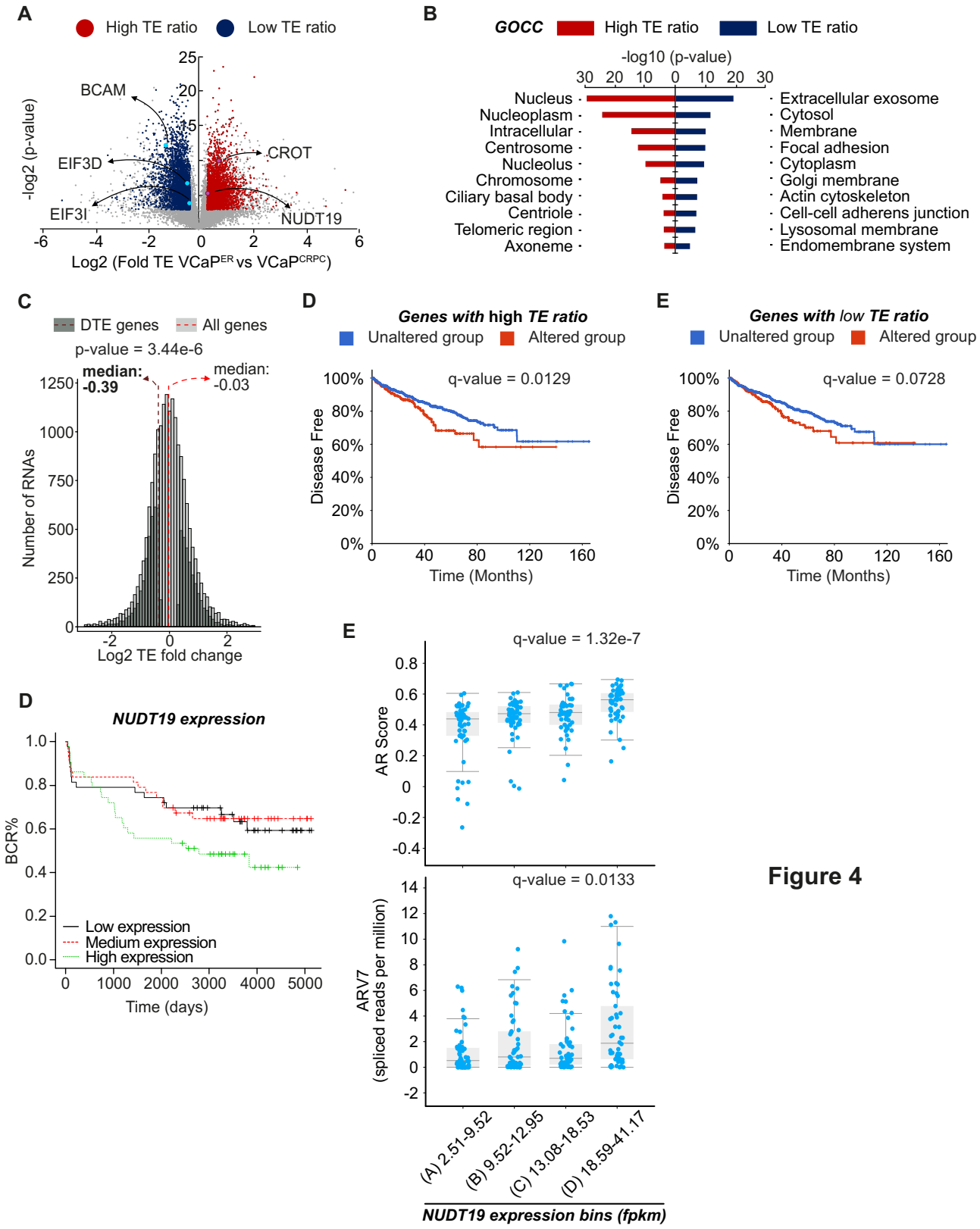
A
High TE ratio
Low TE ratio
BCAM
EIF3D
EIF3I
CROT
NUDT19
-log2 (p-value)
Log2 (Fold TE VCaP^ER vs VCaP^CRPC)
B
GOCC
High TE ratio
Low TE ratio
-log10 (p-value)
Nucleus
Nucleoplasm
Intracellular
Centrosome
Nucleolus
Chromosome
Ciliary basal body
Centriole
Telomeric region
Axoneme
Extracellular exosome
Cytosol
Membrane
Focal adhesion
Cytoplasm
Golgi membrane
Actin cytoskeleton
Cell-cell adherens junction
Lysosomal membrane
Endomembrane system
C
DTE genes
All genes
p-value = 3.44e-6
median: -0.39
median: -0.03
Number of RNAs
Log2 TE fold change
D
Genes with high TE ratio
Unaltered group
Altered group
q-value = 0.0129
Disease Free
Time (Months)
E
Genes with low TE ratio
Unaltered group
Altered group
q-value = 0.0728
Disease Free
Time (Months)
D
NUDT19 expression
BCR%
Low expression
Medium expression
High expression
Time (days)
E
q-value = 1.32e-7
AR Score
q-value = 0.0133
ARV7 (spliced reads per million)
(A) 2.51-9.52
(B) 9.52-12.95
(C) 13.08-18.53
(D) 18.59-41.17
NUDT19 expression bins (fpkm)

Figure 4

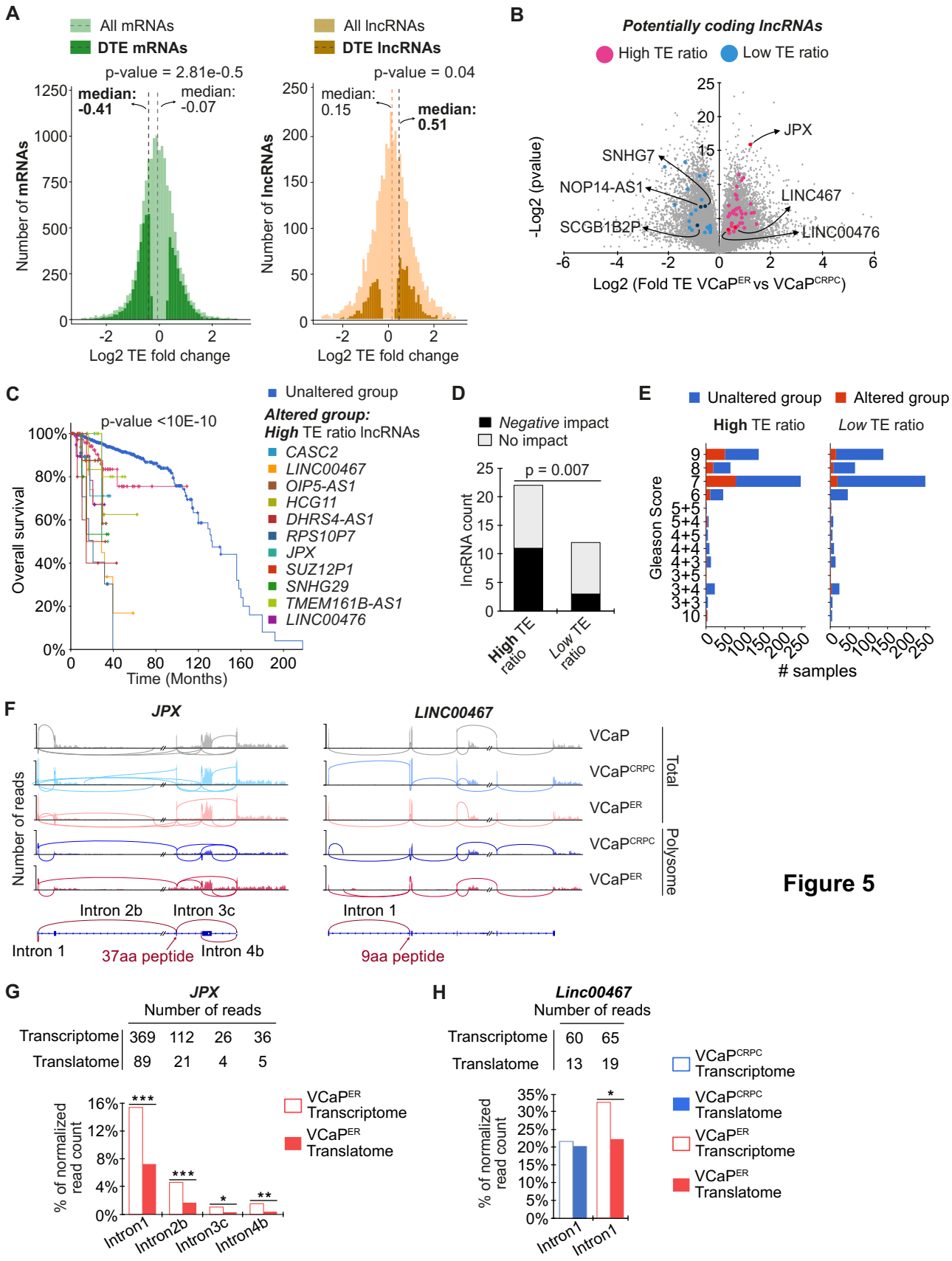
A
All mRNAs
DTE mRNAs
p-value = 2.81e-0.5
median: -0.41
median: -0.07
Number of mRNAs
Log2 TE fold change
All lncRNAs
DTE lncRNAs
p-value = 0.04
median: 0.15
median: 0.51
Number of lncRNAs
Log2 TE fold change
B
Potentially coding lncRNAs
High TE ratio
Low TE ratio
JPX
SNHG7
NOP14-AS1
LINC467
SCGB1B2P
LINC00476
-Log2 (pvalue)
Log2 (Fold TE VCaP^ER vs VCaP^CRPC)
C
p-value <10E-10
Unaltered group
Altered group:
High TE ratio lncRNAs
CASC2
LINC00467
OIP5-AS1
HCG11
DHRS4-AS1
RPS10P7
JPX
SUZ12P1
SNHG29
TMEM161B-AS1
LINC00476
Overall survival
Time (Months)
D
Negative impact
No impact
p = 0.007
lncRNA count
High TE ratio
Low TE ratio
E
Unaltered group
Altered group
High TE ratio
Low TE ratio
Gleason Score
samples
F
JPX
LINC00467
Number of reads
VCaP
VCaP^CRPC
VCaP^ER
Total
Polysome
Intron 2b
Intron 3c
Intron 1
Intron 4b
37aa peptide
9aa peptide
G
JPX
Number of reads
Transcriptome 369 112 26 36
Translatome 89 21 4 5
% of normalized read count
VCaP^ER Transcriptome
VCaP^ER Translatome
Intron1
Intron2b
Intron3c
Intron4b
H
Linc00467
Number of reads
Transcriptome 60 65
Translatome 13 19
% of normalized read count
VCaP^CRPC Transcriptome
VCaP^CRPC Translatome
VCaP^ER Transcriptome
VCaP^ER Translatome
Intron1
Intron1

Figure 5

Figure S1

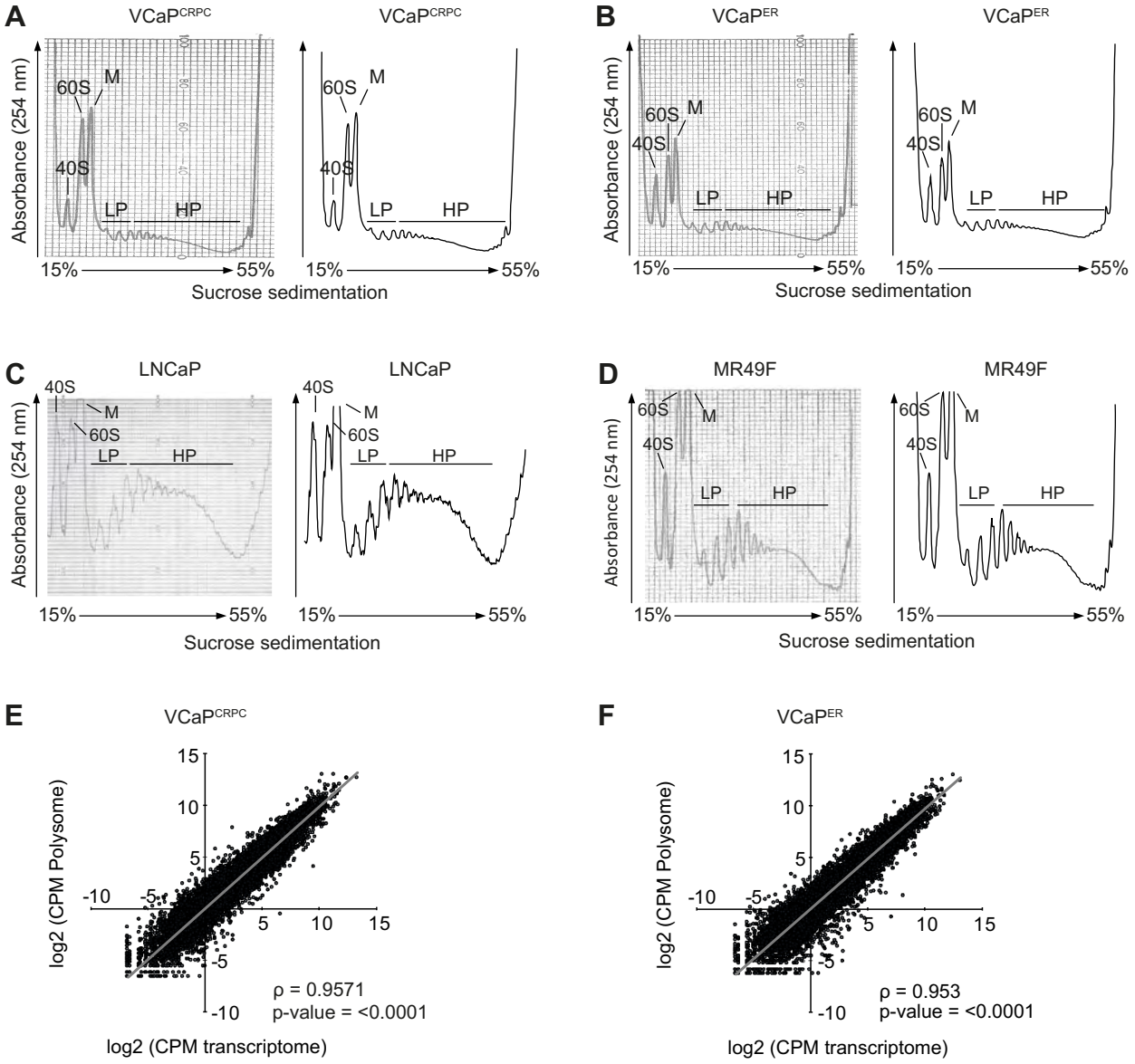
A
VCaP^CRPC
VCaP^CRPC
Absorbance (254 nm)
60S
M
40S
LP
HP
15%
55%
Sucrose sedimentation
B
VCaP^ER
VCaP^ER
C
LNCaP
LNCaP
D
MR49F
MR49F
E
VCaP^CRPC
log2 (CPM Polysome)
log2 (CPM transcriptome)
ρ = 0.9571
p-value = <0.0001
F
VCaP^ER
ρ = 0.953
p-value = <0.0001

Figure S2

A

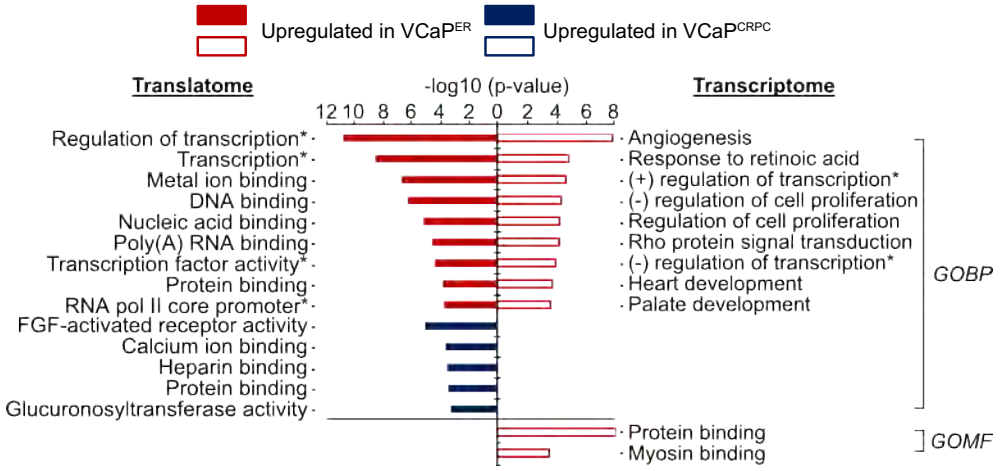

B

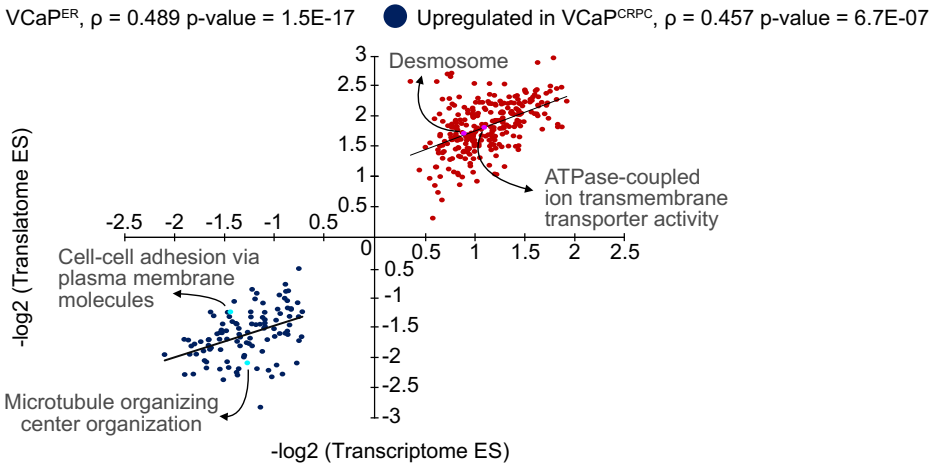

C ***Gene sets enriched in Polysomes VCaP^ER***

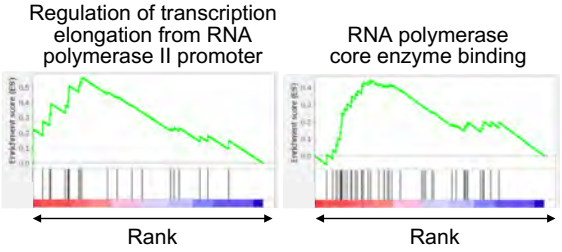

D ***Gene sets enriched in Polysomes VCaP^CRPC***

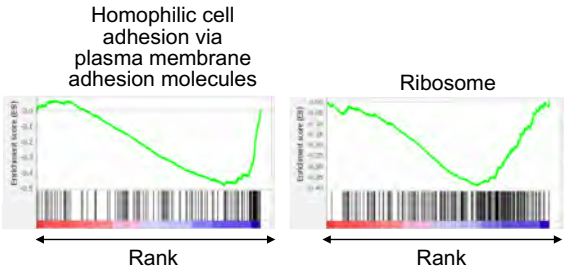

E ***Gene sets enriched in Total RNA VCaP^ER***

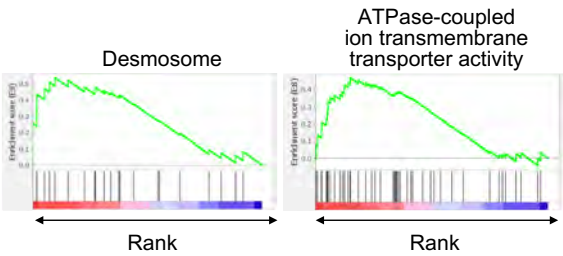

F ***Gene sets enriched in Total RNA VCaP^CRPC***

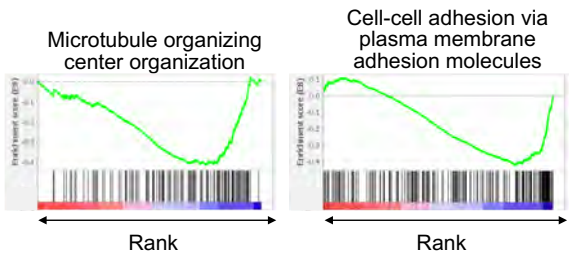

Figure S3

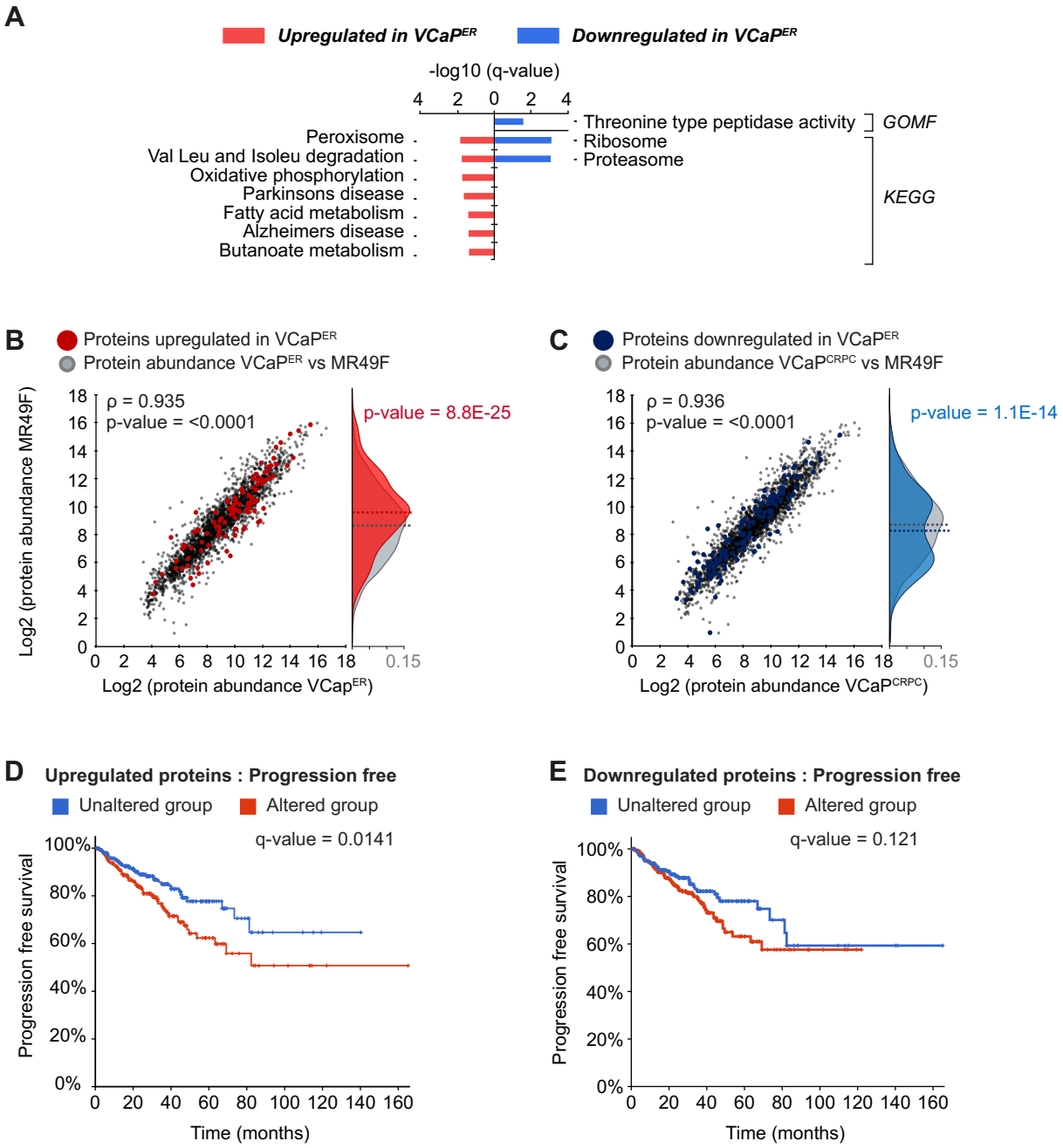
A
Upregulated in VCaP^ER
Downregulated in VCaP^ER
-log10 (q-value)
4 2 0 2 4
Threonine type peptidase activity
Ribosome
Proteasome
GOMF
Peroxisome
Val Leu and Isoleu degradation
Oxidative phosphorylation
Parkinsons disease
Fatty acid metabolism
Alzheimers disease
Butanoate metabolism
KEGG
B
Proteins upregulated in VCaP^ER
Protein abundance VCaP^ER vs MR49F
ρ = 0.935
p-value = <0.0001
p-value = 8.8E-25
Log2 (protein abundance MR49F)
Log2 (protein abundance VCap^ER)
0.15
C
Proteins downregulated in VCaP^ER
Protein abundance VCaP^CRPC vs MR49F
ρ = 0.936
p-value = <0.0001
p-value = 1.1E-14
Log2 (protein abundance VCaP^CRPC)
0.15
D
Upregulated proteins : Progression free
Unaltered group
Altered group
q-value = 0.0141
Progression free survival
Time (months)
E
Downregulated proteins : Progression free
Unaltered group
Altered group
q-value = 0.121
Progression free survival
Time (months)

Figure S4

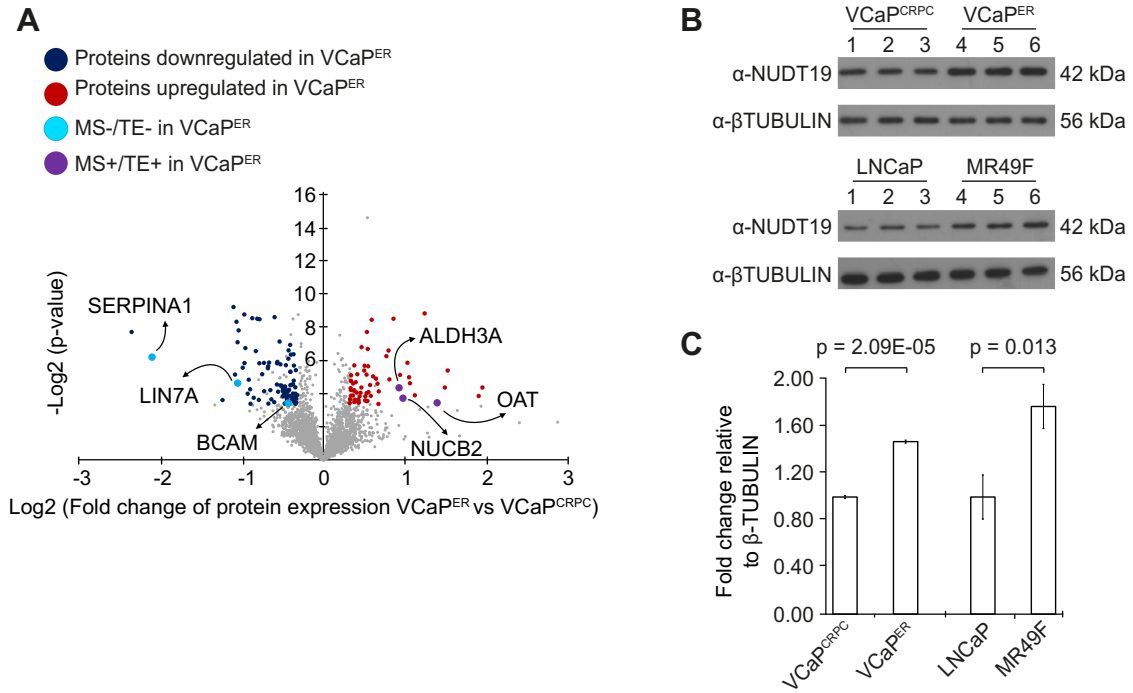
A
Proteins downregulated in VCaP^ER
Proteins upregulated in VCaP^ER
MS-/TE- in VCaP^ER
MS+/TE+ in VCaP^ER
-Log2 (p-value)
SERPINA1
LIN7A
BCAM
ALDH3A
OAT
NUCB2
Log2 (Fold change of protein expression VCaP^ER vs VCaP^CRPC)
B
VCaP^CRPC
VCaP^ER
1 2 3 4 5 6
α-NUDT19
42 kDa
α-βTUBULIN
56 kDa
LNCaP
MR49F
1 2 3 4 5 6
α-NUDT19
42 kDa
α-βTUBULIN
56 kDa
C
p = 2.09E-05
p = 0.013
Fold change relative to β-TUBULIN
VCaP^CRPC
VCaP^ER
LNCaP
MR49F

Figure S5

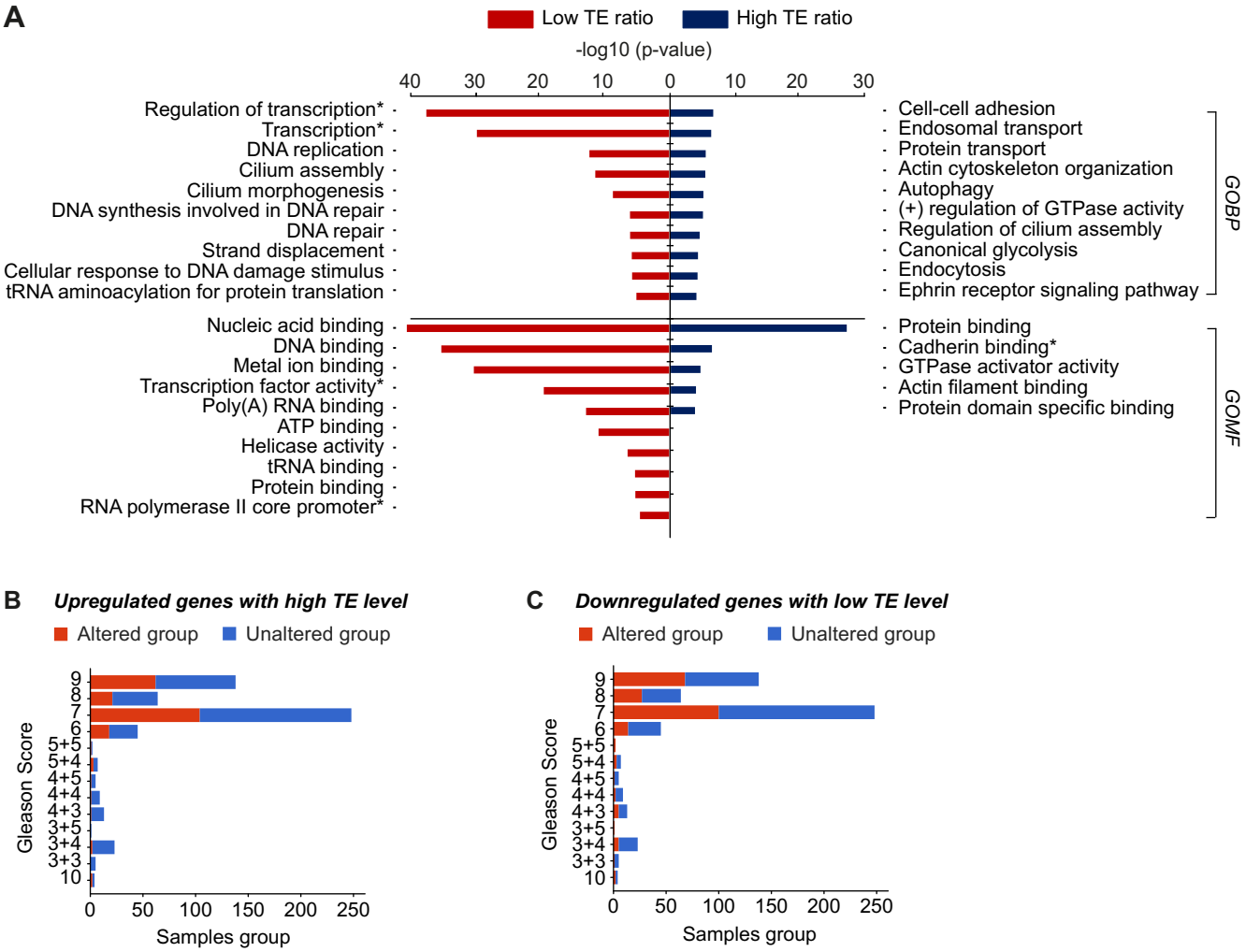
A
Low TE ratio
High TE ratio
-log10 (p-value)
40 30 20 10 0 10 20 30
Regulation of transcription*
Transcription*
DNA replication
Cilium assembly
Cilium morphogenesis
DNA synthesis involved in DNA repair
DNA repair
Strand displacement
Cellular response to DNA damage stimulus
tRNA aminoacylation for protein translation
Cell-cell adhesion
Endosomal transport
Protein transport
Actin cytoskeleton organization
Autophagy
(+) regulation of GTPase activity
Regulation of cilium assembly
Canonical glycolysis
Endocytosis
Ephrin receptor signaling pathway
GOBP
Nucleic acid binding
DNA binding
Metal ion binding
Transcription factor activity*
Poly(A) RNA binding
ATP binding
Helicase activity
tRNA binding
Protein binding
RNA polymerase II core promoter*
Protein binding
Cadherin binding*
GTPase activator activity
Actin filament binding
Protein domain specific binding
GOMF
B
Upregulated genes with high TE level
Altered group
Unaltered group
Gleason Score
9 8 7 6 5+5 5+4 4+5 4+4 4+3 3+5 3+4 3+3 10
0 50 100 150 200 250
Samples group
C
Downregulated genes with low TE level
Altered group
Unaltered group
Gleason Score
9 8 7 6 5+5 5+4 4+5 4+4 4+3 3+5 3+4 3+3 10
0 50 100 150 200 250
Samples group

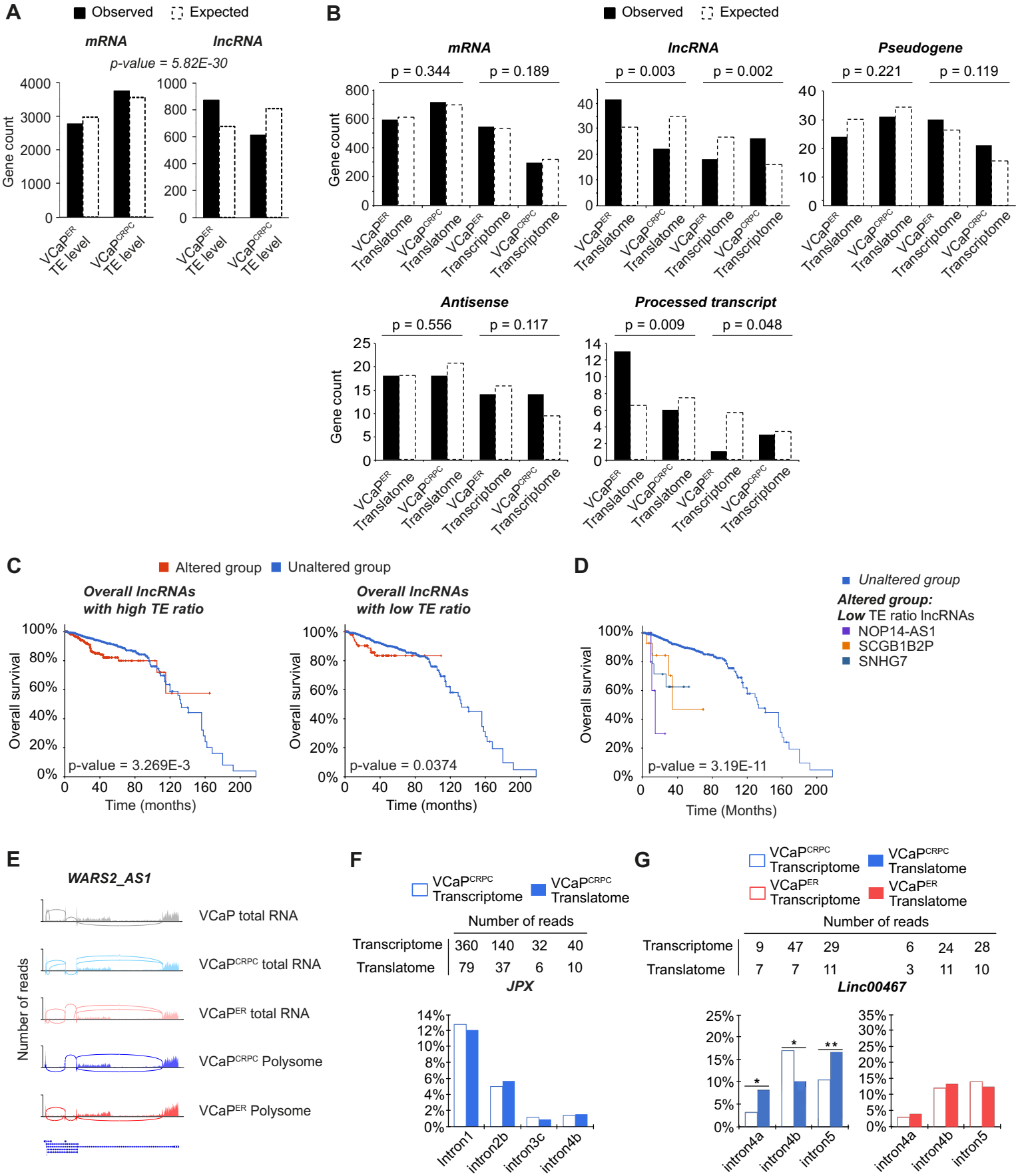
A
Observed
Expected
mRNA
lncRNA
p-value = 5.82E-30
Gene count
VCaPER TE level
VCaPCRPC TE level
B
mRNA
lncRNA
Pseudogene
Antisense
Processed transcript
p = 0.344
p = 0.189
p = 0.003
p = 0.002
p = 0.221
p = 0.119
p = 0.556
p = 0.117
p = 0.009
p = 0.048
VCaPER Translatome
VCaPCRPC Translatome
VCaPER Transcriptome
VCaPCRPC Transcriptome
C
Altered group
Unaltered group
Overall lncRNAs with high TE ratio
Overall lncRNAs with low TE ratio
Overall survival
p-value = 3.269E-3
p-value = 0.0374
Time (months)
D
Unaltered group
Altered group:
Low TE ratio lncRNAs
NOP14-AS1
SCGB1B2P
SNHG7
p-value = 3.19E-11
Time (Months)
E
WARS2_AS1
Number of reads
VCaP total RNA
VCaPCRPC total RNA
VCaPER total RNA
VCaPCRPC Polysome
VCaPER Polysome
F
VCaPCRPC Transcriptome
VCaPCRPC Translatome
Number of reads
Transcriptome 360 140 32 40
Translatome 79 37 6 10
JPX
Intron1
intron2b
intron3c
intron4b
G
VCaPCRPC Transcriptome
VCaPCRPC Translatome
VCaPER Transcriptome
VCaPER Translatome
Number of reads
Transcriptome 9 47 29 6 24 28
Translatome 7 7 11 3 11 10
Linc00467
intron4a
intron4b
intron5

Figure S6